

ODOYO, ISAIAH O., M.S. Optimization of Ambuic Acid as an Anti-Virulence Agent Against Methicillin-Resistant *Staphylococcus aureus*. (2020)  
Directed by Dr. Nadja B. Cech. 46 pp.

Drug resistant bacterial infections are an increasing threat to human health across the globe. Current treatment options for combating these infections primarily rely on antibiotics. Overreliance on the antibiotic therapy continues to accelerate the increase in multi-drug resistant infections. Methicillin-Resistant *Staphylococcus aureus* (MRSA) is amongst the most notorious antibiotic resistant bacterial pathogens. Besides MRSA infections being difficult to treat, they also lead to complications in patient care resulting in extended hospital stays and recurrent visit to the doctors. This imposes a hefty burden on the economy. To address this public health challenge, alternative therapeutic strategies that mitigate proliferation of antibiotic resistance are crucial. A promising approach that is currently pursued as an alternative strategy against bacterial infections is to target bacterial pathogenesis. Pathogenesis in *Staphylococcus aureus* is controlled by a cell density-dependent regulatory (quorum sensing) system also known as the accessory gene regulator (*agr*) system. The *agr* system activates the upregulation of virulence factors that allows the bacteria to thrive in a host. Virulence factors refer to the sum of all the adaptations and compounds produced by an organism that contributes to how well it thrives in a host. Targeting the highly conserved binding sites of the *agr* system is a promising target for broad-spectrum anti-bacterial drugs. One of the compounds that has been reported to inhibit the *agr* system is ambuic acid, a secondary metabolite produced by the fungus *Pestalotiopsis microspora*. Extracts from this fungus exhibit quorum-quenching activity, but the relationship between compound structure and inhibitory

activity of the *agr* system has not been established. To further the goal of developing an innovative countermeasure for MRSA infections that does not drive resistance and can be translated into approved therapeutics, the study seeks to identify additional analogs of ambuic acid that will provide insight into the relationship between chemical structure and quorum sensing inhibitory activity.

To accomplish this goal, growth and extraction of *Pestalotiopsis microspora* fungal cultures were optimized in this study. To facilitate expeditious identification of known compounds in the extract and prioritize isolation of new novel analogs, hyphenated methods combining advanced chromatographic separation techniques, such as ultra-high-performance liquid chromatography coupled to high-resolution mass spectrometry, have been used. The mass spectrometry data set was subjected to mass defect filtering for identification of putative analogs. Nuclear magnetic resonance spectroscopy has been used to profile and characterize the structures of ambuic acid, and its related analogs isolated from the complex extracts. For evaluation of the inhibitory effect of the extracts on the *agr* system, production of the signaling molecule was investigated in a clinically relevant isolate of MRSA (LAC USA 300) cultured with the fungal extracts at two concentrations.

The outcome of this study has been the identification of putative ambuic acid analogs that will provide a starting point for semi-synthetic studies to generate more analogs for further studies on the relationship between chemical structures and quorum sensing inhibitory activity. These studies will provide the much-needed insight to inform

the developments of countermeasure for MRSA infections to augment the use of antibiotics.

OPTIMIZATION OF AMBUIC ACID AS AN ANTI-VIRULENCE AGENT AGAINST  
METHICILLIN-RESISTANT *STAPHYLOCOCCUS AUREUS*

by

Isaiah O. Odoyo

A Thesis Submitted to  
the Faculty of The Graduate School at  
The University of North Carolina at Greensboro  
in Partial Fulfillment  
of the Requirements for the Degree  
Master of Science

Greensboro  
2020

Approved by

---

Committee Chair

To my wife, Erin, for her steadfast support and encouragement. Also, to my parents and family for always encouraging my aspirations.

APPROVAL PAGE

This thesis is written by ISAIAH O. ODOYO, has been approved by the following committee of the Faculty of The Graduate School at The University of North Carolina at Greensboro.

Committee Chair \_\_\_\_\_  
Nadja B. Cech, Ph.D.

Committee Members \_\_\_\_\_  
Nicholas H. Oberlies, Ph.D.

\_\_\_\_\_  
Mitchell P. Croatt, Ph.D.

\_\_\_\_\_  
Daniel A. Todd, Ph.D.

\_\_\_\_\_  
Huzefa A. Raja, Ph.D.

\_\_\_\_\_  
Date of Acceptance by Committee

\_\_\_\_\_  
Date of Final Oral Examination

## ACKNOWLEDGEMENTS

I would like to express my gratitude to my research mentor, Dr. Nadja Cech, for her outstanding mentorship. In her lab, I have received training, guidance, support and developed an appreciation for mass spectrometry. She has imparted in me valuable insights into experimental designs and data analysis. I must also acknowledge my colleagues in Cech Lab for their collaboration, support, and friendship.

In addition, I would like to thank Dr. Joshua Kellogg who introduced me to fungal extraction and bioassay analysis, as well as training and supporting me during the early stages of this project. I am grateful to Dr. Daniel Todd who has taught me to uphold high standards of excellence and thoroughness in mass spectrometry experimentation and analysis.

I would like to acknowledge Dr. Nicholas Oberlies for his guidance and especially for allowing me access to the resources and expertise in his lab. From Oberlies Lab, I must thank Dr. Huzefa Raja for growing and maintaining all the fungal cultures used in this study as well as Sonja Knowles and Tyler Graf for their generosity with their time and knowledge.

As a member of my committee, I am very grateful to Dr. Mitchell Croatt for his time, candid advice, and guidance especially regarding spectroscopic data analysis and presentation.

Finally, I am grateful to the faculty, staff and colleagues in the Chemistry and Biochemistry Department at University of North Carolina at Greensboro for their support and the opportunity to learn, research and study.

## TABLE OF CONTENTS

	Page
LIST OF TABLES .....	vi
LIST OF FIGURES .....	vii
CHAPTER	
I. INTRODUCTION .....	1
II. METHODS .....	9
General Methods .....	9
Isolating Ambuic Acid from Cultures of <i>P. microspora</i> .....	9
UHPLC-MS Analysis of the Fungal Extracts .....	12
NMR Spectroscopy .....	13
Quorum Sensing Inhibition Bioassay .....	14
UHPLC-MS Analysis of the Bacterial Spent Medium .....	15
Mass Defect Filtering .....	15
III. RESULTS AND DISCUSSION .....	17
Ambuic Acid Production by <i>Pestalotiopsis microspora</i> .....	17
AIP-I Inhibition Assay .....	21
Identification of Analogs Through Mass Defect Filtering .....	27
IV. CONCLUSION .....	33
REFERENCES .....	35
APPENDIX A. SUPPLEMENTARY DATA .....	39

## LIST OF TABLES

	Page
Table 1. Crude Extract Masses and Ambuic Acid Yield from <i>P. microspora</i> Batch Extractions .....	11
Table 2. Calculating Ambuic Acid's Deprotonated Molecular Ion .....	18
Table 3. Tabulated Comparative List of the Proton ( <sup>1</sup> H) Assignments .....	20
Table 4. Putative Analog Identification .....	28

## LIST OF FIGURES

	Page
Figure 1. The <i>agr</i> System in <i>Staphylococcus aureus</i> .....	5
Figure 2. Identification of Ambuic Acid in <i>P. microspora</i> Extracts .....	19
Figure 3. MRSA Growth Curves .....	23
Figure 4. AIP-I Percent Inhibition in MRSA.....	24
Figure 5. Fractionation Workflow Chart .....	26
Figure 6. Chromatograms Showing Ambuic Acid and a Putative Analog.....	29
Figure 7. MRSA Growth Curves for Fraction 54-I to 54-VI.....	31
Figure 8. Bioactivity of Fractions 54-I to 54-VI.....	32

## CHAPTER I

### INTRODUCTION

Antibiotic resistance - the ability of germs to overcome the drugs formulated to kill them- is one the greatest challenges facing global health today.<sup>1-3</sup> Even though the full global impact of antimicrobial resistance is difficult to quantify, because of the exiguity of epidemiological data in many parts of the world, the available data portends significant risk to human health.<sup>2,3</sup> The U.S. Center for Disease Control and Prevention's *2019 Antibiotic Resistance Threats Report* (CDC's 2019 AR Threats Report) underscores the continued threat of antibiotic resistance in the Unites States. More than 2.8 million antibiotic-resistant infections occur each year, resulting in loss of more than 35,000 lives, and encumbering the country with a steep economic burden.<sup>1</sup>

One of the pathogens that has been classified as a serious threat to public health and requires a prompt and sustained action is Methicillin-Resistant *Staphylococcus aureus* (MRSA). According to the aforementioned CDC 2019 AR Threats Report, over three hundred thousand patients' hospitalization is attributed to MRSA infection, resulting in more than ten thousand deaths and 1.7 billion attributable healthcare costs in 2017.<sup>1</sup>

*Staphylococcus aureus* is a gram-positive bacteria that primarily exists as a commensal organism and colonizes mucosal membranes and epithelial surfaces of the host.<sup>4-8</sup> It is estimated that greater than 30 percent of the healthy adult population is

colonized with *Staphylococcus aureus*<sup>6</sup>. Although *S. aureus* is more likely to establish its presence as a commensal microbe, it has the potential of becoming pathogenic and causes many systemic diseases and infections ranging from skin infections to life-threatening illnesses.<sup>3,7,9</sup>

Pathogenesis in *Staphylococcus aureus* is controlled by a cell density dependent regulatory system known as quorum sensing, which results in activation of virulence factors.<sup>5-13</sup> Virulence factors refer to the sum of all adaptations and compounds produced by an organism that contribute to how well it thrives in a host.<sup>4,6,7</sup> These factors consist of enzymes, bacterial toxins, cell surface proteins that mediate bacterial attachment, and cell surface carbohydrates and proteins that protect the bacterium.<sup>6</sup> By employing a coordinated and density dependent expression of the genes encoding these virulence factors, bacteria can adapt to the environment in the host and improve their chances of invading and infecting the host.<sup>7</sup>

While the discovery and development of antibiotics has provided great relief and allowed for great advancement in modern medicine, emergence of antibiotic resistant pathogens threatens to turn back this advancement. With current treatment options still relying on antibiotics, dependence on and overuse of antibiotics continues to accelerate the increase in multi-drug resistant (MDR) infections. Methicillin-Resistant *Staphylococcus aureus* (MRSA), are among the first MDR antibiotic resistant bacterial pathogen.<sup>2,4</sup> While antibiotics still provide much needed treatment for bacterial infections, new strategies for augmenting their use is needed. One of the promising strategies for combating antibiotic resistance is to target the pathogenesis mechanism of

the invading bacteria without exerting selective pressure for development of resistance.<sup>3,10,13</sup> Suppressing virulence and thus the ability of bacteria to adapt under varying environmental conditions represents a novel strategy to attenuate infections caused by both gram-negative and gram-positive bacteria.<sup>6,10,13,14</sup>

In *S. aureus*, the expression of virulence factors, responsible for the invasive infection, is mediated by the *accessory gene regulator (agr)* operon.<sup>8,15-17</sup> As outlined in **Figure 1**, the *agr*-system is known to contain two divergent transcripts, RNAII and RNAIII, which are under the control of the P2 and P3 promoters, respectively.<sup>6,14,18</sup> The P3 transcript is a 517-nucleotide designated as RNAIII and is the effector of the *agr*-response. Once expressed, RNAIII initiates the production of a diverse conglomeration of virulence factors that promulgates a broad range of physiological activities including evading host defenses, adhering to cells and tissue matrix, spreading within the host and to degrade cells and tissues, for both nutrition and protection.<sup>7,14</sup> The RNAII transcript covers a four-gene operon (*agrB*, *D*, *C*, and *A*), which encodes for the cytosolic, transmembrane, and extracellular components of the density-sensing two-component signal transduction system. The *agrD* transcript, AgrD, is a short precursor peptide that includes the sequence of the quorum sensing autoinducer, referred to as the autoinducing peptide (AIP).<sup>13,17,18</sup> The processing of AgrD into a functional AIP is primarily mediated by AgrB.<sup>8,13,15,17,19</sup> Upon AgrD binding, AgrB cleaves the C-terminus of AgrD prior to catalyzing thioesterification of the C-terminal carboxylate with the thiol moiety of a conserved cysteine, which is separated from the C-terminal by four amino acid residues.<sup>15,17,19</sup> Lastly, the type I signal peptidase SpsB completes the N-terminal

cleavage of AgrD, releasing a functional AIP from the cell surface.<sup>8,14,18</sup> Secreted AIP then binds the receptor histidine kinase, AgrC, on the bacterial surface, resulting in phosphorylation and activation of the transcription factor, AgrA. In turn, AgrA binds the divergent promoters of the operon, P2 and P3, resulting in continued expression of the four protein components of the operon (via P2) as well as expression of RNAIII (via P3).

Disruption of the *agr*-signaling is a promising strategy to combat invasive *S. aureus* infections.<sup>3,8,10,12,14,15,19,20</sup> Small molecules that inhibit this system, referred to as 'quorum quenchers', target the AgrC, AgrA or AgrB. Of these, AgrC has been the subject of most research and development, and its extracellular location and function as the AIP receptor makes it a prime target for research consideration.<sup>10,13,14</sup> However, AgrC has shown signs of being prone to mutation and may potentially be a site of future resistance development.<sup>13</sup> By contrast, AgrA and AgrB are highly conserved among the *Staphylococci* and even other gram-positive pathogens.<sup>8,13</sup> At present, ambuic acid, a novel organic acid present in isolates of the fungal genus *Pestalotiopsis*, including *Pestalotiopsis microspora*, is the only *bona fide* inhibitor of *agrB*, even though its precise mechanisms of action or even the binding location has yet to be determined.<sup>3,13-15,21,22</sup>

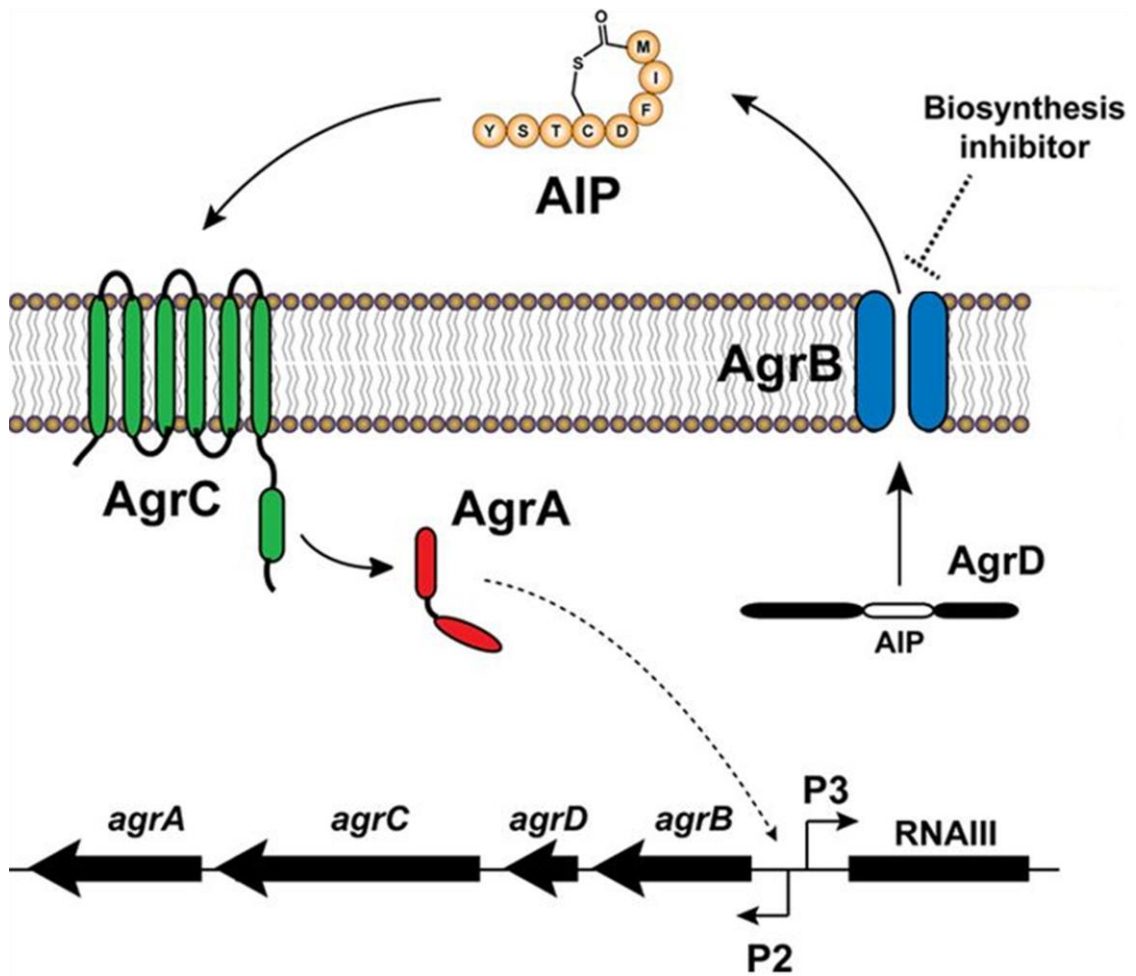


**Figure 1. The *agr*-System in *Staphylococcus aureus*.** The activity of this system is initiated when AIP binds to AgrC, which in turn induces phosphorylation of AgrA, activating the P2 and P3 promoters. The P3 promoter regulates the downstream production of virulence factors that are associated with the pathogenicity of *S. aureus* infections. Activation of the P2 promoter causes transcription of the genes that encode for the components of the *agr*-system, thereby acting as a positive feedback loop that further induces the production of virulence factors. AgrB is responsible for signal biosynthesis, cyclization, and secretion of AgrD precursor as AIP. Ambuic acid (biosynthesis inhibitor) is the only known *agrB* inhibitor. Reproduced with permission from Daniel A. Todd, Corey P. Parlet, Heidi A. Crosby, Cheryl L. Malone, Kristopher P. Heilmann, Alexander R. Horswill, Nadja B. Cech. Copyright 2017 American Society for Microbiology.

Compounds from natural sources, as well as their synthetic derivatives, are highly relevant in medicine today comprising over 70 percent of approved anti-infective drugs.<sup>16,23,24</sup> Approximately one quarter of these natural product derived therapeutics were first isolated from fungi.<sup>16,24</sup> Recent studies have identified fungal metabolites with antivirulence activity against *S. aureus*, including ambuic acid, a secondary metabolite from the endophytic fungi, *Pestalotiopsis microspora*, an Ascomycetes fungus belonging to the order Xylariales.<sup>15,21,23,25,26</sup> Some of the published studies have established the inhibitory activity of ambuic acid on the quorum sensing signal biosynthetic pathway in gram-positive bacteria.<sup>13,15,21,22,25,26</sup> For instance, in the *in vivo* study by Todd *et al.*, a single 25 µg prophylactic dose of ambuic acid was shown to almost fully treat skin ulcer formation, while a 5-µg dose reduced MRSA-induced abscess formation in a murine model by half.<sup>13</sup> Additionally, ambuic acid treatment caused significantly less infection-induced morbidity.<sup>3,13,14</sup>

Ambuic acid is a highly functionalized cyclohexanone which was first isolated from endophytes of tropical rainforest plants after several extracts were observed to display antivirulence activity against *Enterococcus faecalis*.<sup>15,21,23</sup> Ambuic acid, so named in acknowledgment and recognition of the area in Papua New Guinea where the perfect stage of *P. microspora* was first discovered, leading to completion of the description of the life cycle of the organism.<sup>21</sup>

With the promising results from these studies, there has been a growing interest in identifying additional analogs of ambuic acid with similar, if not better, activity that can provide insight into structure activity relationship for this compound. One of the most

efficient techniques used to aid the identification and prioritization of isolation of analogues is mass defect filtering.<sup>27-30</sup>

Mass defect filtering is a post-acquisition mass spectrometry data filtering technique that identifies ions that are within a defined mass defect window around that of the compound of interest based on the assumption that compounds with similar chemical formulas (and thus similar mass defects) will be structurally similar.<sup>30,31,27</sup> The term mass defect is defined as the difference between integer mass and the exact mass of the most abundant isotope in a molecule. The principle of isotopic abundance, that each element contributes to this exact mass and the mass defect, is exploited through definition of a filter placed on the full scan mass spectra data to isolate ions that only fall within a user-defined window around the precursor mass. Mass defect filtering (MDF) of complex MS data has been applied for the selective detection of compounds of interest, including drugs, their metabolites, endogenous ingredients, and naturally occurring plant metabolites.<sup>27,28,30,31</sup>

Inhibition of bacterial pathogenesis is the foundation of the anti-virulence approach that is the focus of the studies presented here. Mass defect filtering provides a rapid screening tool to direct fractionation or exclude fractions from a complex fungal extract by preselecting specific compounds to minimize the number of bioassays that must be performed.

One of the two main aims in this study is to implement an efficient approach by using mass spectrometry data to augment bioassay-directed fractionation in identification and isolation of ambuic acid and its related analogs. This will aid the investigations of the

relationship between their chemical structure and quorum sensing inhibitory activity. The knowledge gained by the described studies supports development of ambuic acid as a novel anti-virulence agent against Methicillin-Resistant *Staphylococcus aureus*.

## CHAPTER II

### METHODS

#### **General Methods**

All solvents and chemicals used were of reagent, spectroscopic or microbiological grade as required and obtained from either Sigma-Aldrich (St. Louis, MO, USA) or ThermoFisher Scientific (Waltham, MA, USA). A reference standard of ambuic acid (AG-CN2-0129-M001, Adipogen Corp. San Diego, CA) was purchased and used in the comparative analysis studies.

Flash chromatography separations were accomplished using an automated CombiFlash RF system (Teledyne-ISCO, Lincoln, NE, USA) and monitored with a PDA detector and an evaporative light scattering detector (ELSD). HPLC separations were performed on a Varian HPLC system (Agilent Technologies, Santa Clara, CA, USA) with Galaxie Chromatography Workstation software (version 1.9.3.2, Agilent Technologies). Analytical HPLC separations employed a Gemini-NX C18 column (5  $\mu\text{m}$ , 110 Å, 250  $\times$  4.60 mm, while preparative-scale HPLC separations were achieved with a 250  $\times$  21.20 mm column; (Phenomenex, Torrance, CA, USA).

#### **Isolating Ambuic Acid from Cultures of *P. microspora***

To identify and isolate ambuic acid and its structurally related analogs produced by the *P. microspora*, fungal cultures grown on oatmeal solid-state media underwent extraction and purification to isolate the secondary metabolites. To permit scaled up

purification of target compounds, separate batch extractions was conducted for a total of 52 Erlenmeyer flasks (10 g of oatmeal per 250 mL flask). Oatmeal media (Old fashioned Quaker oats) was prepared using 10 g of rolled oats in each 250 mL Erlenmeyer flask with approximately 17 mL of deionized-H<sub>2</sub>O, followed by autoclaving at 221 °C for 30 minutes using previously outlined methods.<sup>32</sup> The batch extractions included a total of 52 flasks; the total weight of the extracts and number of flasks per batch are as outlined in **Table 1**.

Each batch extraction of cultures was achieved by addition of 60 mL of (1:1) MeOH-CHCl<sub>3</sub> into each 250 mL flask, chopping thoroughly with a spatula, and shaking overnight (~16 hours) at ~100 rpm at 22°C. The organic mixture was then filtered on a Büchner funnel under vacuum and a mixture of 90 mL CHCl<sub>3</sub> and 150 mL H<sub>2</sub>O (per flask) added to the filtrate. Subsequently, the mixture was then stirred for 30 minutes using a magnetic stir bar and transferred into a separatory funnel. The organic layer (CHCl<sub>3</sub>) was drawn off and evaporated to dryness *in vacuo*. The dried organic layer was reconstituted in 60 mL of (1:1) MeOH-CH<sub>3</sub>CN and 60 mL of Hexane per flask, transferred into a separatory funnel and shaken vigorously. The defatted organic layer (MeOH-CH<sub>3</sub>CN) was evaporated to dryness *in vacuo* and the resulting complex extract transferred into pre-weighed 20 mL scintillation vial and dried under nitrogen and designated as the starting material (SM).

**Table 1. Crude Extract Masses and Ambuic Acid Yield from *P. microspora* Batch Extractions.** Fractions obtained from SM-002, SM-003 and SM-004 were pooled to isolate ambuic acid, and the same process was conducted with fractions from SM-005, SM-006, and SM-007.

Starting Material	Number of Flasks	Resulting Extract Mass (mg)	Ambuic Acid Yield (mg)	Ambuic Acid Yield (mg)/flask
G910-18012-9 (SM-002)	6	696.84	49.4	2.74
G910-18012-29 (SM-003)	6	1278.77		
G910-18012-31 (SM-004)	6	807.51		
G910-18012-33 (SM-005)	8	960.89	29.2	1.22
G910-18012-35 (SM-006)	6	657.06		
G910-18012-37 (SM-007)	10	1252.83		

An aliquot of three separate biological replicate extracts from *P. microspora*, SM-002, SM-003 and SM-004 were combined and designated as G190-18012-54, making a total of 2.4 grams. Similarly, extracts SM-005, SM-006 and SM-007 were combined for a total of 2.247 g. Each combined batch of extracts was then separately subjected to fractionation to isolate ambuic acid. The combined defatted extracts were dissolved in minimal volume of CHCl<sub>3</sub>, absorbed onto Celite 545 (Acros Organics), and fractionated by normal phase flash chromatography using a gradient of Hexane-CHCl<sub>3</sub>-MeOH at a 40 mL/minute flow rate and 53.0 column volumes ( **Figure 5**). For the combined material from SM-002, SM-003, and SM-004, six fractions were collected and designated as

G910-18012-54-I through G910-18012-54-VI (**Figure S6**). This was repeated for SM-005, SM-006 and SM-007, and designated as G910-18012-75 (**Figure S7**).

Purification was achieved via preparative HPLC and was conducted from pooled fractions 54-IV and 54-V from SM-002, SM-003 and SM-004 using a gradient system with starting conditions at 20:80 CH<sub>3</sub>CN-H<sub>2</sub>O with 0.1 % formic acid and gradually ramped to 100:0 CH<sub>3</sub>CN-H<sub>2</sub>O with 0.1 % formic acid over 30 minutes at a flow rate of 16.9 mL/minutes. Purification was conducted for fractions 54-IV and 54-V with a total starting mass of 465.85 mg. As a result, 49.41 mg of ambuic acid were isolated. This process was repeated for fractions 75-IV and 75-V from SM-005, SM-006 and SM-007, respectively. From this group of fractions, a total mass of 29.17 mg of ambuic acid was isolated.

### **UHPLC-MS Analysis of the Fungal Extracts**

To detect ambuic acid and its structurally related analogs from the *P. microspora* cultures, the fungal extracts were dissolved in Optima grade methanol to obtain a final concentration of 100 µg·mL<sup>-1</sup>. Chromatographic separation was performed on an Acquity Ultra-Performance Liquid Chromatography (UPLC) system (Waters, Milford, MA) equipped with an autosampler kept at 10°C, photodiode array detector (PDA), column manager and a binary solvent manager, interfaced to a Thermo LTQ Orbitrap XL mass spectrometer with an electrospray ionization (ESI) source. Injections of 3 µL were performed on an Acquity UPLC BEH C<sub>18</sub> column set at 40°C (1.7 µm, 2.1 x 50mm, Waters) with a flow rate of 0.3 mL/min using a binary solvent gradient of water (0.1% formic acid added) and acetonitrile (0.1% formic acid added): linear gradient of 15-85 %

Acetonitrile over 10 minutes. The negative ionization mode of the mass spectrometer was utilized over a full scan of  $m/z$  120-1200 with the following settings: capillary voltage 5 V, capillary temperature, 300 °C, sheath gas ( $N_2$ ) and auxiliary gas flow rate, 48 and 11 units respectively. The data dependent MS/MS events were performed on the most intense ions detected in full scan MS. The full scans were acquired at a resolution of 35,000 fwhm while the  $MS^2$  scans were acquired at 17,500 fwhm. The MS/MS isolation window width was 2 Daltons, and the normalized collision energy (NCE) set to 40 units. Each sample was injected in triplicate to provide analytical replicates for analysis.

A standard of ambuic acid was analyzed at  $50 \mu\text{g}\cdot\text{mL}^{-1}$  to obtain the characteristic retention time. After optimal separation was accomplished, extract samples were analyzed, and compounds were identified by matching retention times and exact mass to those of the standard on Xcalibur (v. 3.0.63. Thermo Fisher Scientific).

### **NMR Spectroscopy**

For NMR studies, samples were prepared by dissolving the purified extract fractions from the crude organic extracts in 450  $\mu\text{L}$   $\text{CD}_3\text{Cl}$  or  $\text{CD}_3\text{OD}$  then transferring to 5 mm 7" NMR tubes. Proton NMR analysis was mostly carried out on a JEOL ECS 400 MHz spectrometer system equipped with a high sensitivity JEOL Royal probe (NM-03810R05). Some of the studies were done on a JEOL ECA 500 MHz spectrometer. Spectra were processed using MestReNova (Mnova v. 11.0.1-17801, Mestrelab Research SL, US) software.

### **Quorum Sensing Inhibition Bioassay**

For this study, a wild type strain of methicillin-resistant *Staphylococcus aureus* (MRSA), USA 300 LAC (AH1263), provided by Dr. Alex Horswill Lab, University of Colorado, Anschutz Medical Campus, was used.

A single isolated colony inoculum of the MRSA (LAC USA300) strain established on Mueller- Hinton broth was grown overnight in Tryptic Soy Broth (Sigma Aldrich, St. Louis, MO) at 37°C for 24 hours with shaking at 200 rpm in a New Brunswick Scientific shaker/incubator series I-26. Overnight cultures were then diluted to 1:200 (culture: broth) and shaken at 200 rpm at 37°C for two hours, at which point the OD<sub>600</sub> was measured to be in the range of 0.08-0.1.

A 96 well tissue culture treated flat bottom plate (Corning Incorporated) was inoculated with 245 µL of this diluted bacterial inoculum and 5 µL of inhibitor or control in each well. Ambuic acid (Adipogen life Sciences), was used as an inhibitor, and was prepared at two concentrations, 10 µg·mL<sup>-1</sup> and 100 µg·mL<sup>-1</sup>, respectively. Stock solutions of ambuic acid and various fractions were prepared in DMSO and assay content of DMSO was 2% in all wells. Assays were performed in triplicate for each treatment and control. The vehicle control consisted of 2% DMSO. The plate was incubated at 37 °C and shaken at 1000 rpm in a Stuart Microtitre Shaker Incubator (SI505). OD<sub>600</sub> was measured at 1 hr. intervals using a Synergy H1 Plate Reader and the experiment was considered complete at OD<sub>600</sub> of 2.0 (~4-6 hrs.). At completion of the incubation time, the culture broth containing bacteria was transferred to a clear sterile 96-well, 0.22 µm

hydrophilic plate, with low protein binding durapore membrane (MultiScreen®) and filtered under vacuum. The spent media were then analyzed by UPLC-MS.

### **UHPLC-MS Analysis of the Bacterial Spent Medium**

An Acquity UPLC system (Waters, Corporation, Milford, MA) coupled to an LTQ-Orbitrap XL hybrid mass spectrometer (Thermo Fisher Scientific, Waltham, MA) was used for UHPLC-MS analyses. For the samples collected in the 5 hr. growth analysis, a 3  $\mu$ L injection of each sample was eluted from the column (Acquity UPLC BEH C18 1.7  $\mu$ m, 2.1 x 50 mm, Waters Corporation) at a flow rate of 0.3 mL/min with solvent A consisting of water (Optima LC-MS grade) with 0.1% formic acid added and solvent B consisting of methanol (Optima LC-MS grade). The gradient was initiated with an isocratic composition of 80:20 (A:B) for 0.5 min, increasing linearly from 0.5 min to 6.00 min to 20:80 (A:B) followed by an isocratic hold for 0.1 min. From 6.10-7.10 min the gradient increased linearly to 0:100 with a 0.5 min isocratic hold. The gradient returned to initial starting conditions from 7.50-8.00 min and was held for 0.5 min. The mass spectrometer was operated in positive ionization mode for the scan range of 150-1500 with the following settings: capillary voltage of 44V, capillary temperature of 350 °C, tube lens offset of 50 V, spray voltage of 3.80 kV, sheath gas flow at 35 units, and auxiliary gas at 30 units.

### **Mass Defect Filtering**

Identification of ambuic acid analogs was achieved through processing of the collected accurate mass spectra of the fractionated extracts from the high-resolution mass spectrometers on the Thermo Scientific Compound Discoverer software 2.1.0.398.

The negative ion mode LC-MS data acquired from the Q Exactive Plus were analyzed, aligned, and filtered with the MS<sup>1</sup> detected ions subjected to formula prediction using the following parameters from the workflow nodes: lower RT limit 3, upper RT limit 7, minimum precursor ion mass of 100 Da and maximum, 5000 Da. The maximum tolerance of mass error set at 5 ppm: H-C ratio was below 5; RDBE (degree of unsaturation) was defined at max of 40, noise level at  $1.0 \times 10^3$  counts, mass tolerance of 500 Da and mass defect tolerance of 50 mDa for the specified elemental composition of C<sub>19</sub>H<sub>26</sub>O<sub>6</sub>.

## CHAPTER III

### RESULTS AND DISCUSSION

#### **Ambuic Acid Production by *Pestalotiopsis microspora***

Species within the fungal genus *Pestalotiopsis* have attracted research as a commonly isolated endophyte of tropical plants which has been shown to produce a variety of bioactive and structurally complex secondary metabolites.<sup>21,23,33–35</sup> One of the most common *Pestalotiopsis* species is *P. microspora*.<sup>21,23,33,34</sup>

To assess production of ambuic acid and other secondary metabolites in cultures of *P. microspora*, the LC-MS data obtained from the extract were analyzed using the Xcalibur software to create base peak and selected ion chromatograms. The average molecular mass of ambuic acid is 350.4130, calculated from its elemental composition of C<sub>19</sub>H<sub>26</sub>O<sub>6</sub>. The theoretical monoisotopic mass, computed by taking the sum of the accurate masses of the most abundant or primary isotope of each atom in the molecule<sup>28,36</sup>, for ambuic acid is 350.1729. A comparative analysis of the UHPLC-MS data acquired in the negative ion mode yielded evidence of presence of ambuic acid in the extracts. Identification of ambuic acid in the complex extract was achieved through detection of the deprotonated molecular ion [M-H]<sup>-1</sup>. Ambuic acid's deprotonated molecular ion has an *m/z* value of 349.1651, eluting at a retention time of 4.59 minutes. The *m/z* value represents the mass to charge ratio, which is dimensionless because it describes the ratio between the molecular ion mass number (*m*) and the number of

elementary charges ( $z$ ).<sup>36-38</sup> For the deprotonated molecular ion of ambuic acid  $[M-H]^{-1}$ , the  $m/z$  value is arrived at by subtraction of hydrogen's mass number from the monoisotopic mass of ambuic acid, as shown in **Table 2**.

**Table 2. Calculating Ambuic Acid's Deprotonated Molecular Ion**

Ambuic Acid Monoisotopic mass	350.1729
Hydrogen Mass number	1.0078
Deprotonated Ambuic acid $m/z$ value	349.1651

Qualitatively, ambuic acid was confirmed to be present in the extracts by comparison of accurate mass and retention time to that of a standard of ambuic acid. The selected ion chromatograms of two extracts of biological replicates (separate cultures) of *P. microspora*, SM-01 and SM-02, have similar retention times to that of a standard of ambuic acid as illustrated in **Figure 2**. Ambuic acid was determined to be a major component of the complex crude extract and its structure was established after chromatographic separation and purification. Confirmation was achieved by comparison of the chemical shifts and the coupling constants of the proton NMR data of the isolate with the literature reported data<sup>21</sup> as conveyed on **Table 3**.

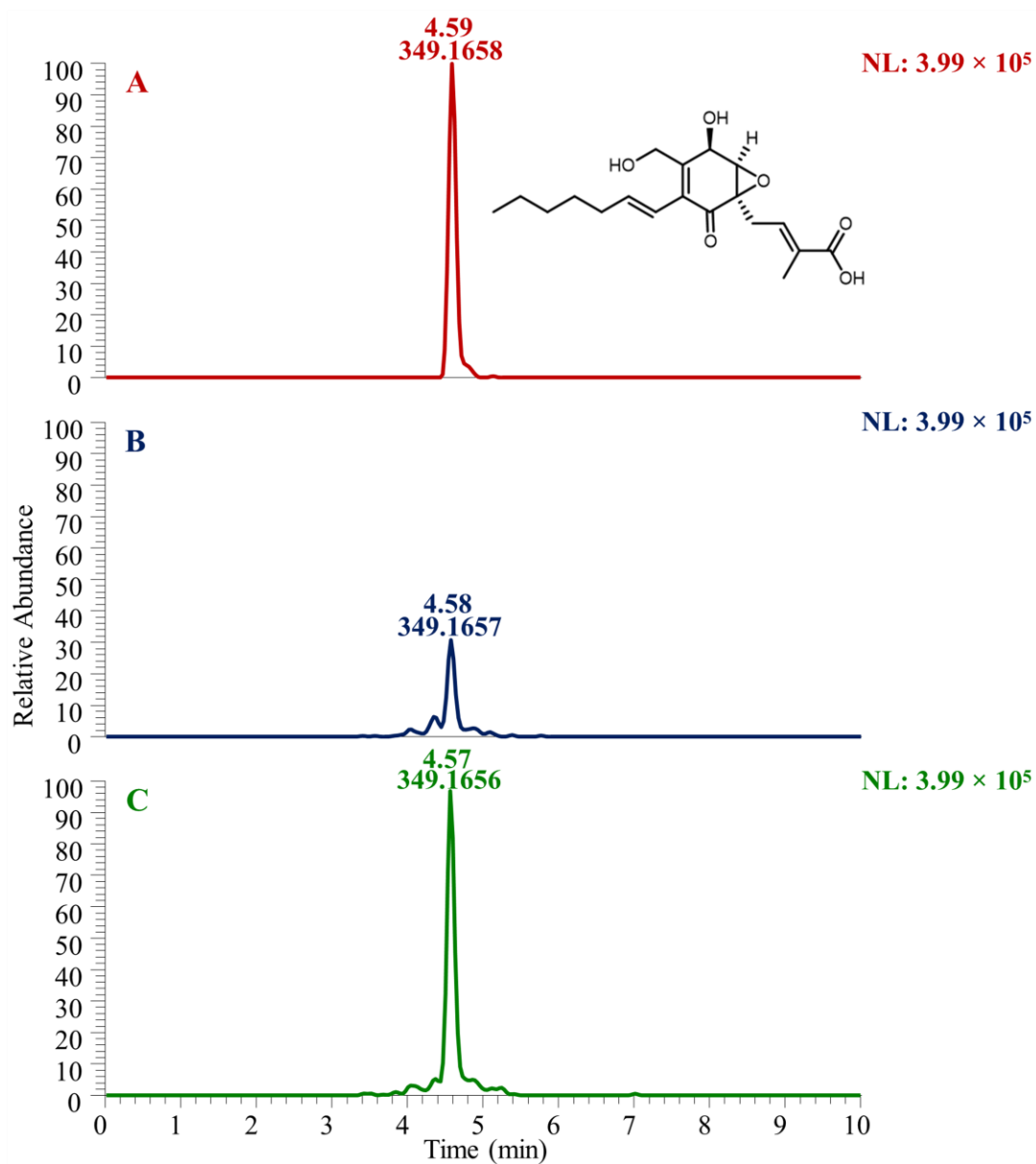


**Figure 2. Identification of Ambuic Acid in *P. microspora* Extracts.** Selected ion chromatograms were constructed for the ambuic acid standard and replicate extracts at an  $m/z$  value of 349.1651,  $[M-H]^{-1}$ , at a retention time of 4.59 minutes, with an isolation window of 5ppm and normalized to  $3.99 \times 10^5$ . The chromatogram in (A) represents a standard of ambuic acid analyzed at a concentration of  $50 \mu\text{g}\cdot\text{mL}^{-1}$ . (B) and (C) were obtained by analysis of two replicate extracts from separate cultures of *P. microspora* at a concentration of  $100 \mu\text{g}\cdot\text{mL}^{-1}$  and are referred to as SM-01 and SM-02. SM- Abbreviation for starting material, representing the two separate extractions of biological replicates of the *P. microspora*.

**Table 3. Tabulated Comparative List of the Proton ( $^1\text{H}$ ) Assignments.** The isolated fraction's  $^1\text{H}$  NMR data was processed using MestReNova software (v. 11.0.1-17801). All reported data were obtained in  $\text{d}_4$ -methanol ( $\text{CD}_3\text{OD}$ ). Ambuic acid isolated from *P. microspora* via preparative HPLC.

Values for ambuic acid from literature				Experimentally measured values for ambuic acid from <i>P. microspora</i>	
Carbon #	$\delta^{13}\text{C}$	$\delta^1\text{H}$	Coupling	$\delta^1\text{H}$	Coupling
1	171.2				
2	131.9				
3	136.6	6.67	<i>t</i> , $J = 7.5$	6.68	<i>t</i> , $J = 7.3$
4	28.8	2.78	<i>q of d</i> , $J = 7.8, 15.8$	2.81	<i>q of d</i> , $J = 7.8, 15.8$
5	61.3				
6	61.1	3.74	<i>d</i> , $J = 2.8$	3.74	<i>d</i> , $J = 2.8$
7	66.0	4.81	<i>s</i>	4.81	<i>s</i>
8	150.7				
9	132.0				
10	196.0				
11	122.8	6.13	<i>d</i> , $J = 15.9$	6.12	<i>d</i> , $J = 15.9$
12	140.3	5.83	<i>m</i>	5.82	<i>m</i>
13	34.6	2.15	<i>q</i> , $J = 7.0$	2.14	<i>q</i> , $J = 7.1$
14	30.0	1.43	<i>m</i>	1.43	<i>m</i>
15	32.6	1.32	<i>m</i>	1.31	<i>m</i>
16	23.6	1.32	<i>m</i>	1.31	<i>m</i>
17	14.5	0.90	<i>t</i> , $J = 6.9$	0.89	<i>t</i> , $J = 6.9$
18	13.0	1.86	<i>s</i>	1.85	<i>s</i>
19	60.3	4.39	<i>d</i> , $J = 12.9$	4.39	<i>d</i> , $J = 12.9$
		4.51	<i>d</i> , $J = 12.9$	4.50	<i>d</i> , $J = 12.9$

### **AIP-I Inhibition Assay**

In order to examine if the inhibitory activity of ambuic acid and analogs resulted in the inhibition of the *agr* quorum sensing system, production of the signaling molecule, auto-inducing peptide-I (AIP-I), was investigated in clinically relevant isolate of MRSA (LAC USA300). The complex extracts (SM-01 and SM-02) representing the starting material, were cultured with bacterial cells and ambuic acid standard at two concentrations, 10  $\mu\text{g}\cdot\text{mL}^{-1}$  and 100  $\mu\text{g}\cdot\text{mL}^{-1}$ . Ambuic acid is hypothesized to inhibit the production of AIP-I through inhibition of AgrB and generally have no antimicrobial growth effect at concentrations below 200  $\mu\text{g}\cdot\text{mL}^{-1}$  <sup>39</sup>. Since AIP production is dependent on cell density, a growth curve was created by tracking cell growth. Growth of cells was measured by turbidity using optical density hourly, for four hours (**Figure 3**). The data suggests that ambuic acid does not inhibit growth of bacteria both at 10  $\mu\text{g}\cdot\text{mL}^{-1}$  and at 100  $\mu\text{g}\cdot\text{mL}^{-1}$ . However, the bacterial cells cultured with the extracts (SM-01 and SM-02) at 100 $\mu\text{g}\cdot\text{mL}^{-1}$  exhibited a suppressive growth effect on MRSA. These are complex extracts and it is likely that some of the constituents in the extracts are responsible for the suppressed growth at 100  $\mu\text{g}\cdot\text{mL}^{-1}$ . With further fractionation and purification, the constituents responsible for the quorum sensing inhibitory activity were separated from the antimicrobial components.

Evaluation of the inhibitory activity of the extracts on the *agr* system was monitored through production of the macrocyclic peptide, AIP-I. This was achieved through qualitative measurement of AIP in the culture filtrate by LC-MS analysis. The quorum sensing cyclic peptide of MRSA, AIP-I, was clearly detected by LC-MS analysis of the culture filtrate. A comparative analysis of the peak area corresponding to AIP-I qualitatively showed a decrease in the peak areas at the two concentrations, 10 $\mu\text{g}\cdot\text{mL}$  and 100 $\mu\text{g}\cdot\text{mL}$ , when this strain was cultured with SM-01 and SM-02 as compared to ambuic

acid standard at the same concentration, **Figure 4**. Both at  $10 \mu\text{g}\cdot\text{mL}^{-1}$  and at  $100\mu\text{g}\cdot\text{mL}^{-1}$ , SM-01 and SM-02 exhibit a comparatively similar AIP-I inhibition as the ambuic acid standard. However, the observed activity is not attributable to ambuic acid alone since both SM-01 and SM-02 exhibited growth inhibition at  $100 \mu\text{g}\cdot\text{mL}^{-1}$ . Collectively, the data presented in **Figures 2-4** demonstrated that the *P. microspora* extracts contained ambuic acid and further suggested that the ambuic acid therein possess quorum sensing inhibition activity. The results for the quorum sensing inhibition assay are somewhat confounded by antimicrobial effects, therefore, it was necessary to carry out further fractionation to separate the putative quorum sensing inhibitors from the antimicrobial constituents in the extracts.

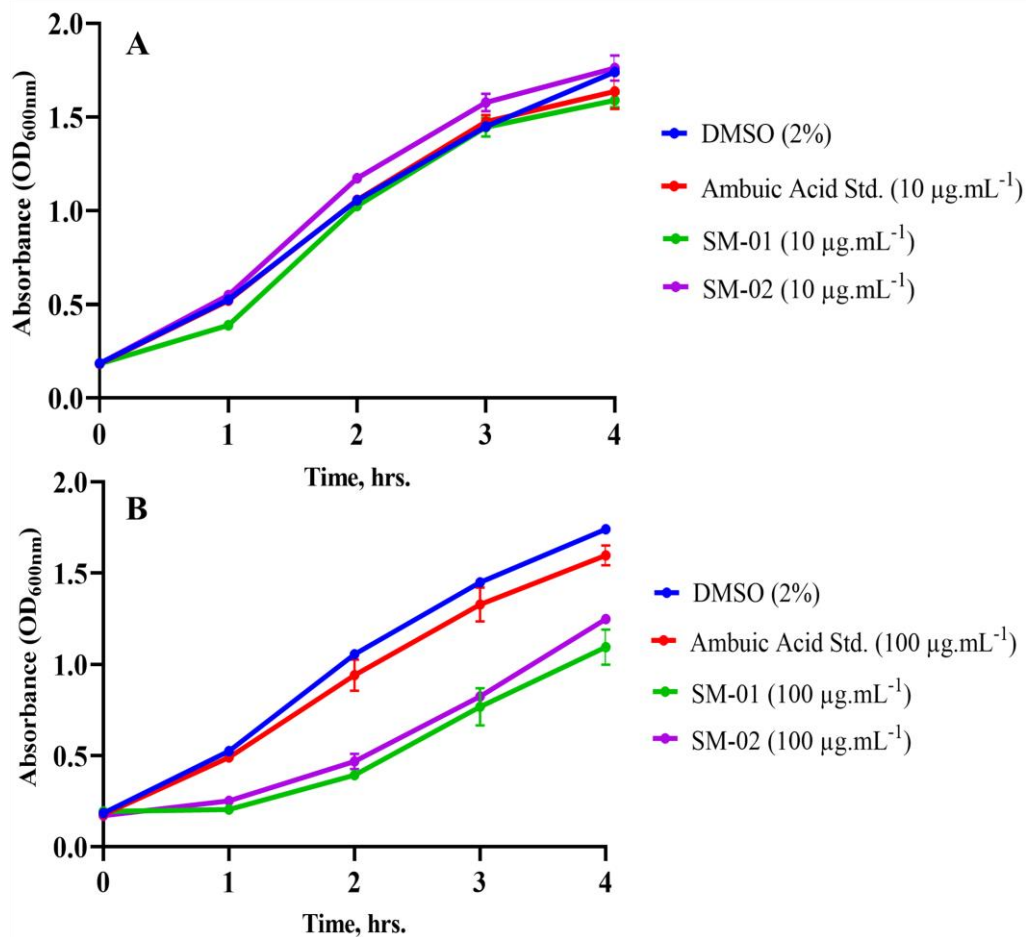


**Figure 3. MRSA Growth Curves.** The growth curves for MRSA USA300 LAC (AH1263) were constructed from turbidimetric measurements at OD<sub>600</sub>. The vehicle consisted of 2% DMSO in tryptic soy broth while ambuic acid standard served as the positive control. Triplicate wells were prepared for the controls and SM-01 and SM-02 and incubated for 4 hours at 37°C and OD<sub>600</sub> measurement were collected hourly. (A) and (B) were obtained by plotting absorbance measurements at 10 µg·mL<sup>-1</sup> and 100 µg·mL<sup>-1</sup>, respectively. Background absorbance was subtracted using wells containing samples without bacteria. Error bars are representative of the standard error of the mean of the triplicates.

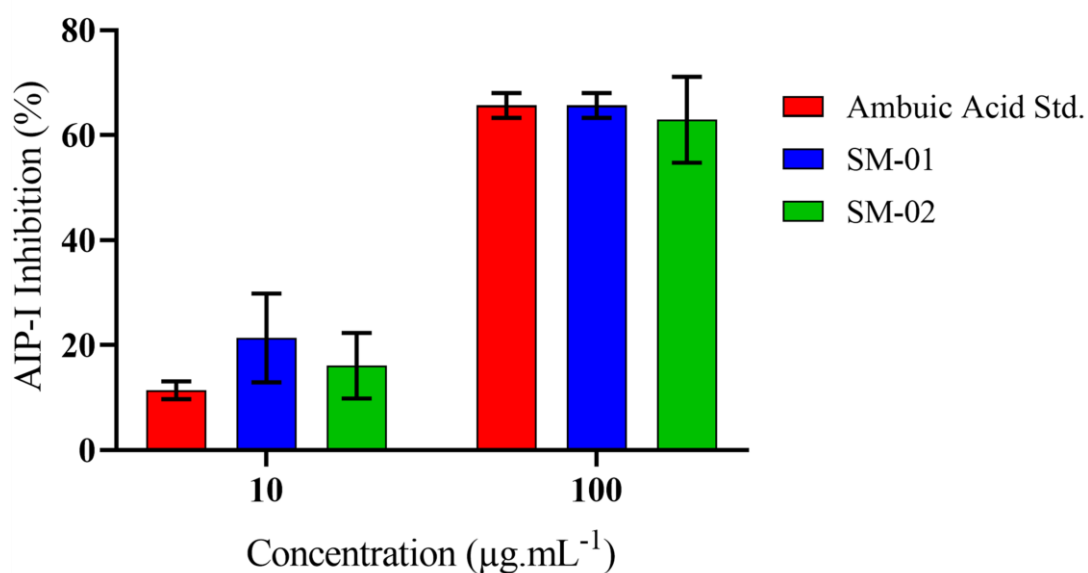


**Figure 4. AIP-I Percent Inhibition in MRSA.** Normalized AIP-I percent inhibition in MRSA by ambuic acid and extracts from *P. microspora*. Peak areas were calculated using Xcalibur software version 3.0.63 and the data exported to Excel for calculation of mean peak areas. AIP-I inhibition was calculated by normalizing to vehicle (2% DMSO). Error bars are representative of the standard error of the mean.

Consequently, three separate biological replicate extracts from *P. microspora*, were combined, designated G910-18012-54, and subjected to flash chromatography. Each batch extract was designated as the starting material and referred to as SM as outlined in the method section. An aliquot of biological replicate extracts SM 002, SM-003 and SM-004 were combined, making a total of 2.4 grams. This was then fractionated and analyzed following the work flowchart depicted in **Figure 5**. A total of six fractions were collected by pooling of the eluates collected under the same peak with 95% recovery, **Figure S6**. Fractions eluting with 80% chloroform/hexanes and 100% methanol were expected to contain ambuic acid and the analogs. Examination of plotted selected ion chromatograms positively confirmed presence of ambuic acid in the fourth (54-IV) and fifth (54-V) fractions. Further isolation of the two fractions (54-IV and 54-V) via preparative HPLC yielded 49.41 milligrams of pure ambuic acid with positive confirmation of the structure achieved through comparison of the observed nuclear magnetic resonance chemical shifts to published data<sup>21</sup> as conveyed on **Table 3** and in **Figures S2** and **S3**. The process was repeated for three other combined replicate extracts, SM 005-007 with a total of 29.17 milligrams of pure ambuic acid isolated. Thus far, a total of 78.58 of pure ambuic acid has been isolated from seven separate batch extractions of cultures of *P microspora*.

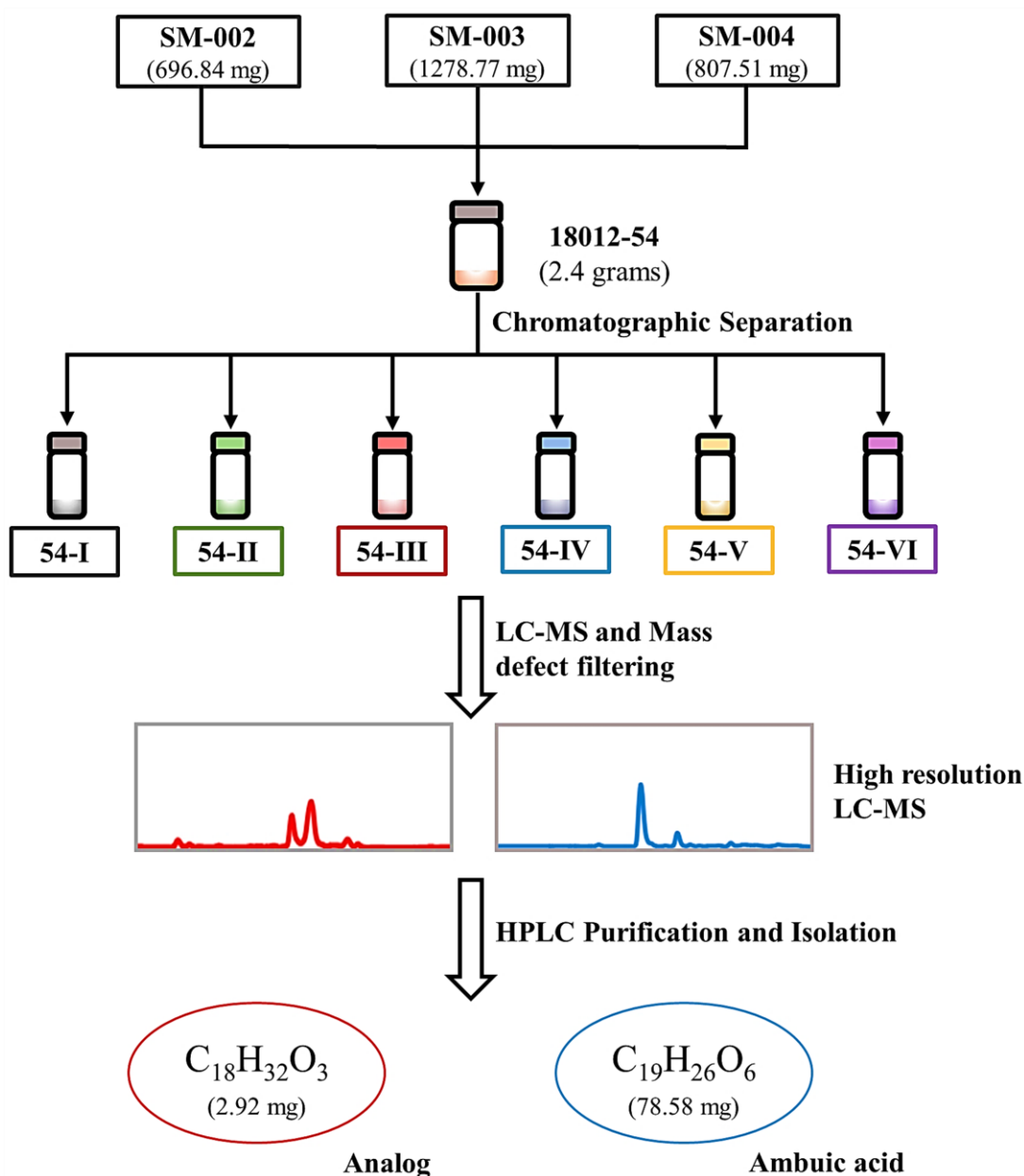


**Figure 5. Fractionation Workflow Chart.** Three biological replicate extracts of *P. microspora* labelled SM-002, SM-003 and SM-004, were combined and designated G910-18012-54. ISCO flash chromatography of the combined replicates yielded six fractions, 54-I through 54-VI. Fractions were analyzed by high resolution mass spectrometry and the resulting data set subjected to mass defect filtering. Fraction 54-III yielded an analog of ambuic acid with predicted formula of C<sub>18</sub>H<sub>32</sub>O<sub>3</sub> while Fraction 54-IV yielded ambuic acid, molecular formula C<sub>19</sub>H<sub>26</sub>O<sub>6</sub>

## Identification of Analogs Through Mass Defect Filtering

Based on the hypothesis that the MRSA quorum sensing inhibitory activity of extracts from the fungus *Pestalotiopsis microspora* is due to the effects of ambuic acid and its analogs on the *agr* signal transduction system that is responsible for pathogenesis and virulence in the bacteria, Compound Discoverer, a qualitative post acquisition data-processing application that uses accurate mass data, isotope pattern matching, and mass spectral library searches, was employed for the structural identification of putative ambuic acid analogs.<sup>30,38</sup> To rigorously characterize these new compounds, the fractions collected from flash chromatography were subjected to mass defect filtering and analyzed for analogs identification. The LC-MS data were subjected to mass defect filtering with a signal threshold set at  $1.0 \times 10^3$  and mass tolerance and mass defect tolerance set at  $\pm 500$  Da and 0.05, respectively. A total of 1175 compounds were identified as having matching patterns indicating all required isotopes of searched pattern were found. Out of these, 1026 were identified as having the predicted compositions as  $C_{19}H_{26}O_6$ , indicating a match between the assigned annotation and the available results. A compound with the molecular formula established as  $C_{18}H_{32}O_3$  on the basis of its HRESIMS ( $m/z$  295.2287,  $[M-H]^{-1}$ ) was identified as the most abundant analog of ambuic acid in the *P. microspora* extracts, falling within a 0.0622 mass defect of ambuic acid, with a nominal mass difference of 54 Da, as outlined in **Table 4**. This putative analog was determined to be in the second (54-II) and third (54-III) fractions of the combined SM-02 to SM-04 biological replicates of *P. microspora* extracts, **Figure 6**.

**Table 4. Putative Analog Identification.** Based on the structure of ambuic acid ( $C_{19}H_{26}O_6$ ), a mass defect filter was defined with the mass tolerance of  $C_{19}H_{26}O_6 \pm 500$  Da and mass defect tolerance of  $\pm 50$  mDa. Mass defect calculated as the difference between the integer mass and the monoisotopic mass of the most abundant isotopes in a molecule.

	Formula Prediction	MW (accuracy in ppm)	RT <sup>a</sup> (Min)	<i>m/z</i> Monoisotopic mass [ M-H] <sup>-1</sup>	Nominal mass [ M-H] <sup>-1</sup>	Mass defect
Ambuic Acid	$C_{19}H_{26}O_6$	350.17382	4.590	349.1651	349	0.1651
Putative Analog	$C_{18}H_{32}O_3$	296.23595	6.080	295.2273	295	0.2273
Difference	1 C, 6 H, 3 O	53.93787	1.49	53.9378	54	0.0622

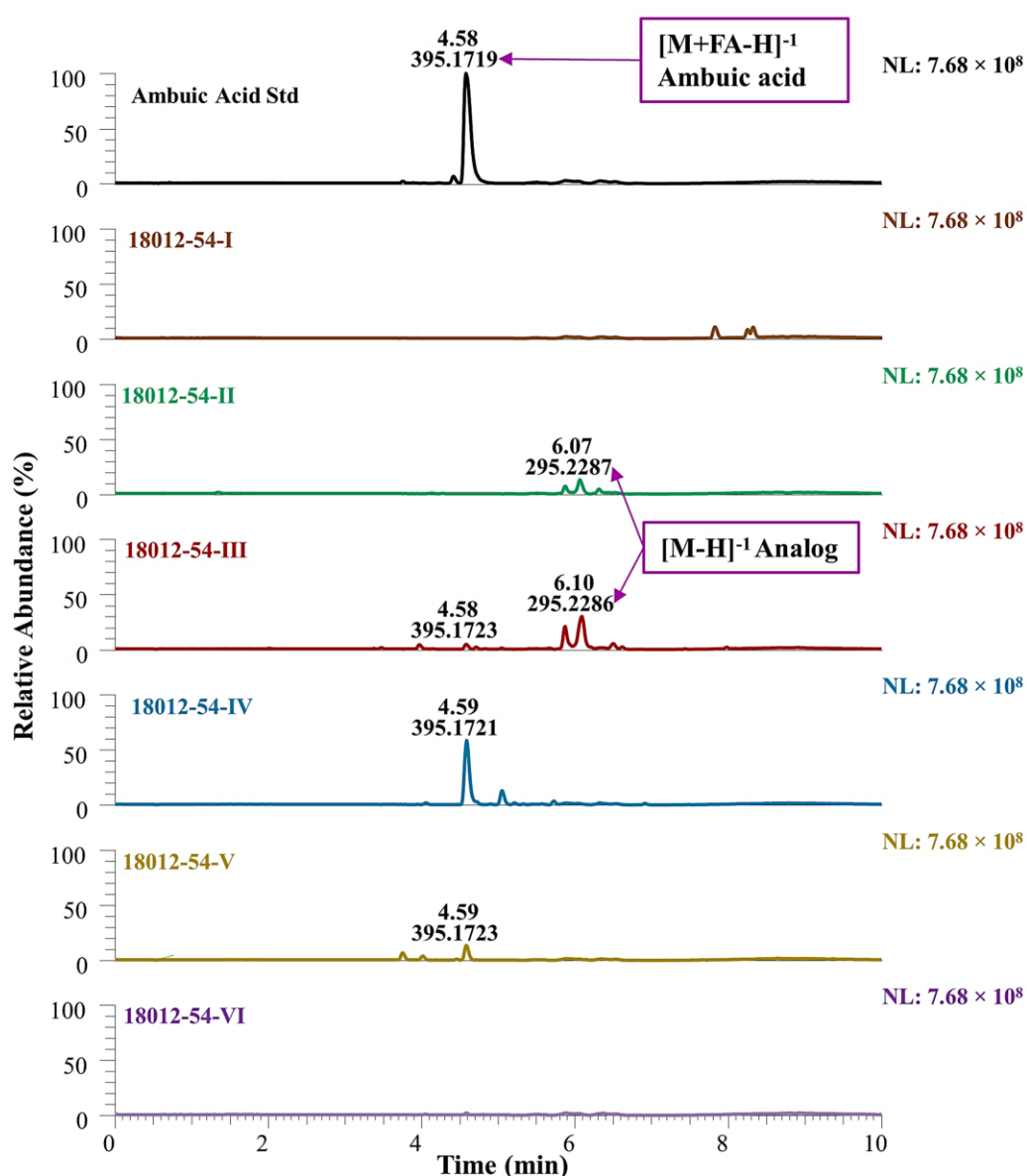


**Figure 6. Chromatograms Showing Ambuic Acid and a Putative Analog.** Base peak chromatograms from the UPLC-MS analysis of the fractions from the combined SM 02-SM-04, highlighting the retention times of ambuic acid's deprotonated molecular ion with a formate adduct  $[M+FA-H]^{-1}$  at 4.58 min and  $m/z$  value of 395.1719 and the putative analog's deprotonated molecular ion  $[M-H]^{-1}$  at retention time range of 5.88-6.10 min and  $m/z$  value 295.2287 plotted with an isolation window of 5 ppm and normalized to  $7.68 \times 10^8$ . The first chromatogram represents a standard ambuic acid analyzed at a concentration of  $50 \mu\text{g}\cdot\text{mL}^{-1}$ . Fractions 54-I through 54-VI were obtained by analysis of the ISCO fractions from fractionation of SM 02-SM-04, from cultures of *P. microspora* analyzed at a concentration of  $100 \mu\text{g}\cdot\text{mL}^{-1}$

Further studies to examine the effect of the putative analog containing fraction on the *agr* quorum sensing system were carried out by investigation of production of the signaling molecule, auto-inducing peptide-I (AIP-I), in clinically relevant isolate of MRSA (LAC USA300) as previously outlined. The results of the study suggest that the analog has inhibitory effect on the AIP-I production without effect on the growth of the bacteria both at  $10\ \mu\text{g}\cdot\text{mL}^{-1}$  and at  $100\ \mu\text{g}\cdot\text{mL}^{-1}$ . Fraction 54-III, the fraction in which the putative analog was identified, shows no growth inhibitory effects at the two concentrations used in the study, **Figure 7**. Analysis of the peak area of AIP-I similarly depicts a reduction in the AIP-I production as compared to the 2% DMSO vehicle control, thus, inferring that the constituents in both fraction 54-II and 54-III inhibit the AIP-I production, **Figure 8**. As a putative analog of ambuic acid, isolated compound with the predicted formula  $\text{C}_{18}\text{H}_{32}\text{O}_3$  will provide additional information for the structure activity relationship studies in relation to quorum quenching activity in MRSA and development and optimization of ambuic acid as an antivirulence agent. Structure elucidation for the compound is ongoing.

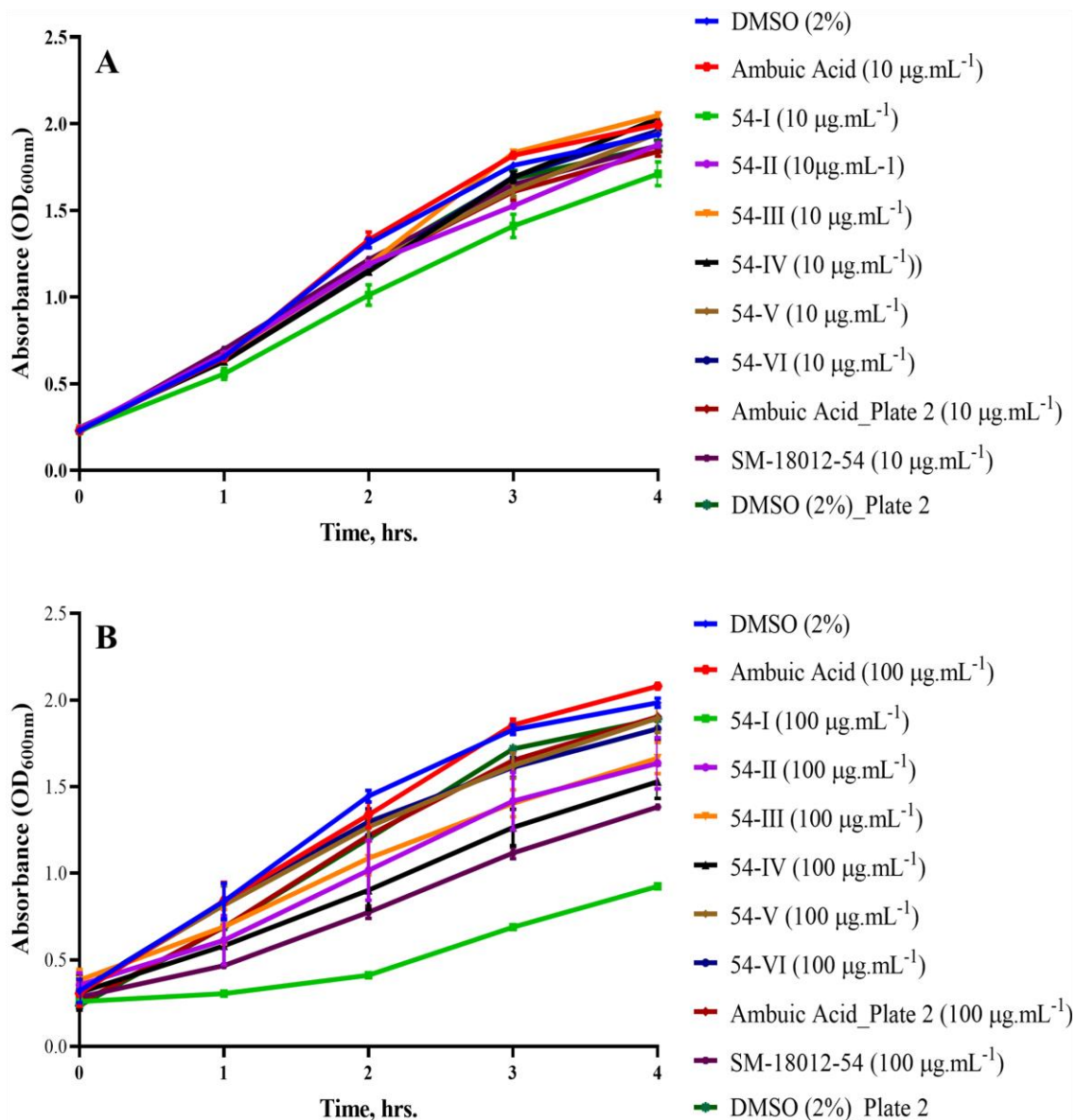


**Figure 7. MRSA Growth Curves for Fraction 54-I to 54-VI.** The growth curves were established from turbidimetric measurements at OD<sub>600</sub>. The vehicle control consisted of 2% DMSO in broth while ambuic acid standard served as positive control. Triplicate wells were prepared for the controls as well as the fractions and incubated for 4 hours at 37°C. (A) and (B) were obtained by plotting absorbance measurements at 10 µg·mL<sup>-1</sup> and 100 µg·mL<sup>-1</sup> respectively. Background absorbance was subtracted using wells containing samples without bacteria and errors bars are representative of the standard error of the mean of the triplicates.

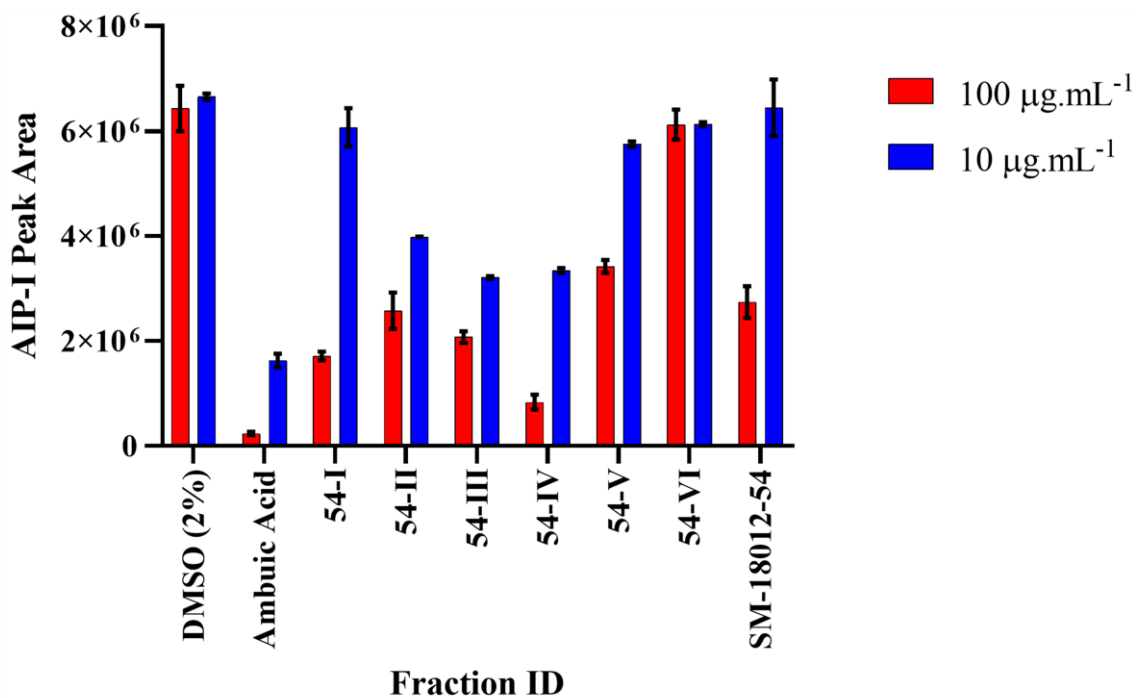


**Figure 8. Bioactivity of Fractions 54-I to 54-VI.** Fractions collected from fractionation of the combined replicate complex extracts (starting materials, SM-02-SM-04) and designated SM-18012-54, were tested for AIP biosynthesis inhibition. Ambuic was used as a positive control for comparative analysis of biological response. SM-18012-54 (the starting material) was tested for comparison. Error bars are representative of the standard error of the mean of the triplicates.

## CHAPTER IV

### CONCLUSION

One of the novel strategies aimed at attenuating progression of infections caused by bacteria is by suppressing their ability to adapt under varying environmental conditions.<sup>14,18,39,40</sup> Research efforts aimed at the discovery and development of small molecule *agr* system inhibitors have yielded some promising leads.<sup>14-16,39</sup> Small molecule inhibitors targeting the most conserved AgrB may be one of the best candidates for therapeutic development and every lead needs to be pursued.

The studies presented here have outlined an optimized method for extraction, purification, and identification of ambuic acid and its related structural analogs from solid media cultures of the fungus *Pestalotiopsis microspora*. A total of 80 milligrams of purified ambuic acid was isolated from 52, 10-gram flasks, in seven different batches of growths. Access to this material will enable further investigations of mechanism of action for this molecule and will provide a starting point for semi-synthetic studies to generate more analogs for structure activity relationship studies.

Recently, mass defect filtering, a technique for detecting both common and unique metabolites, has been utilized for detection of compounds of interest. Traditionally, natural products discovery depended on exhaustive and challenging bioassay-guided fractionation and purification of active constituents, followed by their

identification based on nuclear magnetic resonance (NMR) and mass spectrometry (MS) data. Integrating these technologies in our studies offered a powerful tool capable of identifying putative active compounds in the complex extracts as well as simplifying the process, thus saving costs and time. By combining these technologies, we optimized the isolation protocols for ambuic acid analogs. Mass defect filtering has broad applications to natural products chemistry and will be useful in other natural products discovery programs. This approach accelerated processing of ion mass information and allowed grouping of compounds based on the narrow mass defect, even when their nominal mass difference was significant. Consistent with other recently published studies<sup>28,36,37</sup>, it was found that coupling mass defect filtering with bioassay-directed fractionation offered a complementary process to traditional bioactive compound discovery, focusing on targeted compounds and requiring fewer processing steps as compared to the traditional cycle of fractionation, bioassay, and characterization.

Multidrug resistant pathogens, like MRSA, pose a significant challenge for the currently available clinical care. Therefore, modified use of the available antimicrobial agents and public health interventions, coupled with novel antivirulence strategies, may help in mitigating the effects of the multidrug-resistant organisms in the future.

## REFERENCES

- (1) MRSA | CDC <https://www.cdc.gov/mrsa/index.html> (accessed May 6, 2019).
- (2) Marston, H. D.; Dixon, D. M.; Knisely, J. M.; Palmore, T. N.; Fauci, A. S. Antimicrobial Resistance. *JAMA* **2016**, *316* (11), 1193-1204. <https://doi.org/10.1001/jama.2016.11764>.
- (3) Salam, A. M.; Quave, C. L. Targeting Virulence in Staphylococcus Aureus by Chemical Inhibition of the Accessory Gene Regulator System In Vivo. *mSphere* **2018**, *3* (1), e00500-17. <https://doi.org/10.1128/mSphere.00500-17>.
- (4) Gajdács, M. The Continuing Threat of Methicillin-Resistant Staphylococcus Aureus. *Antibiotics* **2019**, *8* (2), 52. <https://doi.org/10.3390/antibiotics8020052>.
- (5) Rutherford, S. T.; Bassler, B. L. Bacterial Quorum Sensing: Its Role in Virulence and Possibilities for Its Control. *Cold Spring Harb. Perspect. Med.* **2012**, *2* (11), a012427. <https://doi.org/10.1101/cshperspect.a012427>.
- (6) Jenul, C.; Horswill, A. R. Regulation of Staphylococcus Aureus Virulence. *Microbiol. Spectr.* **2019**, *6* (1). <https://doi.org/10.1128/microbiolspec.GPP3-0031-2018>.
- (7) Novick, R. P. Autoinduction and Signal Transduction in the Regulation of Staphylococcal Virulence. *Mol. Microbiol.* **2003**, *48* (6), 1429–1449. <https://doi.org/10.1046/j.1365-2958.2003.03526.x>.
- (8) Tan, L.; Li, S. R.; Jiang, B.; Hu, X. M.; Li, S. Therapeutic Targeting of the Staphylococcus Aureus Accessory Gene Regulator (Agr) System. *Front. Microbiol.* **2018**, *9*. <https://doi.org/10.3389/fmicb.2018.00055>.
- (9) Mediavilla, J. R.; Chen, L.; Mathema, B.; Kreiswirth, B. N. Global Epidemiology of Community-Associated Methicillin Resistant Staphylococcus Aureus (CA-MRSA). *Curr. Opin. Microbiol.* **2012**, *15* (5), 588–595. <https://doi.org/10.1016/j.mib.2012.08.003>.
- (10) Cech, N. B.; Horswill, A. R. Small-Molecule Quorum Quenchers to Prevent *Staphylococcus Aureus* Infection. *Future Microbiol.* **2013**, *8* (12), 1511–1514. <https://doi.org/10.2217/fmb.13.134>.
- (11) Paguigan, N. D.; Rivera-Chávez, J.; Stempin, J. J.; Augustinović, M.; Noras, A. I.; Raja, H. A.; Todd, D. A.; Triplett, K. D.; Day, C.; Figueroa, M.; Hall, P. R.; Cech, N. B.; Oberlies, N. H. Prenylated Diresorcinols Inhibit Bacterial Quorum Sensing. *J. Nat. Prod.* **2019**, *82* (3), 550–558. <https://doi.org/10.1021/acs.jnatprod.8b00925>.
- (12) Asad, S.; Opal, S. M. Bench-to-Bedside Review: Quorum Sensing and the Role of Cell-to-Cell Communication during Invasive Bacterial Infection. *Crit. Care* **2008**, *12* (6), 236. <https://doi.org/10.1186/cc7101>.

- (13) Todd, D. A.; Parlet, C. P.; Crosby, H. A.; Malone, C. L.; Heilmann, K. P.; Horswill, A. R.; Cech, N. B. Signal Biosynthesis Inhibition with Ambuic Acid as a Strategy To Target Antibiotic-Resistant Infections. *Antimicrob. Agents Chemother.* **2017**, *61* (8), e00263-17, /aac/61/8/e00263-17.atom. <https://doi.org/10.1128/AAC.00263-17>.
- (14) Horswill, A. R.; Gordon, C. P. Structure–Activity Relationship Studies of Small Molecule Modulators of the Staphylococcal Accessory Gene Regulator. *J. Med. Chem.* **2019**. <https://doi.org/10.1021/acs.jmedchem.9b00798>.
- (15) Nakayama, J.; Uemura, Y.; Nishiguchi, K.; Yoshimura, N.; Igarashi, Y.; Sonomoto, K. Ambuic Acid Inhibits the Biosynthesis of Cyclic Peptide Quorumones in Gram-Positive Bacteria. *Antimicrob. Agents Chemother.* **2009**, *53* (2), 580–586. <https://doi.org/10.1128/AAC.00995-08>.
- (16) Cragg, G. M.; Newman, D. J. Natural Products: A Continuing Source of Novel Drug Leads. *Biochim. Biophys. Acta BBA - Gen. Subj.* **2013**, *1830* (6), 3670–3695. <https://doi.org/10.1016/j.bbagen.2013.02.008>.
- (17) Sturme, M. H. J.; Kleerebezem, M.; Nakayama, J.; Akkermans, A. D. L.; Vaughan, E. E.; de Vos, W. M. Cell to Cell Communication by Autoinducing Peptides in Gram-Positive Bacteria. 11.
- (18) Thoendel, M.; Kavanaugh, J. S.; Flack, C. E.; Horswill, A. R. Peptide Signaling in the Staphylococci. *Chem. Rev.* **2011**, *111* (1), 117–151. <https://doi.org/10.1021/cr100370n>.
- (19) Zhang, L.; Gray, L.; Novick, R. P.; Ji, G. Transmembrane Topology of AgrB, the Protein Involved in the Post-Translational Modification of AgrD in *Staphylococcus Aureus*. *J. Biol. Chem.* **2002**, *277* (38), 34736–34742. <https://doi.org/10.1074/jbc.M205367200>.
- (20) Bjarnsholt, T.; Givskov, M. Quorum Sensing Inhibitory Drugs as next Generation Antimicrobials: Worth the Effort? *Curr. Infect. Dis. Rep.* **2008**, *10* (1), 22. <https://doi.org/10.1007/s11908-008-0006-y>.
- (21) Li, J. Y.; Harper, J. K.; Grant, D. M.; Tombe, B. O.; Bashyal, B.; Hess, W. M.; Strobel, G. A. Ambuic Acid, a Highly Functionalized Cyclohexenone with Antifungal Activity from *Pestalotiopsis* Spp. and *Monochaetia* Sp. *Phytochemistry* **2001**, *56* (5), 463–468. [https://doi.org/10.1016/S0031-9422\(00\)00408-8](https://doi.org/10.1016/S0031-9422(00)00408-8).
- (22) Zhang, Q.; Luan, R.; Li, H.; Liu, Y.; Liu, P.; Wang, L.; Li, D.; Wang, M.; Zou, Q.; Liu, H.; Matsuzaki, K.; Zhao, F. Anti-inflammatory Action of Ambuic Acid, a Natural Product Isolated from the Solid Culture of *Pestalotiopsis neglecta*, through Blocking ERK/JNK Mitogen-activated Protein Kinase Signaling Pathway. *Exp. Ther. Med.* **2018**. <https://doi.org/10.3892/etm.2018.6294>.
- (23) Strobel, G. A. Endophytes as Sources of Bioactive Products. *Microbes Infect.* **2003**, *5* (6), 535–544. [https://doi.org/10.1016/S1286-4579\(03\)00073-X](https://doi.org/10.1016/S1286-4579(03)00073-X).
- (24) Newman, D. J.; Cragg, G. M. Natural Products as Sources of New Drugs over the Nearly Four Decades from 01/1981 to 09/2019. *J. Nat. Prod.* **2020**, *83* (3), 770–803. <https://doi.org/10.1021/acs.jnatprod.9b01285>.

- (25) Figueroa, M.; Jarmusch, A. K.; Raja, H. A.; El-Elimat, T.; Kavanaugh, J. S.; Horswill, A. R.; Cooks, R. G.; Cech, N. B.; Oberlies, N. H. Polyhydroxyanthraquinones as Quorum Sensing Inhibitors from the Guttates of *Penicillium Restrictum* and Their Analysis by Desorption Electrospray Ionization Mass Spectrometry. *J. Nat. Prod.* **2014**, *77* (6), 1351–1358. <https://doi.org/10.1021/np5000704>.
- (26) Daly, S. M.; Elmore, B. O.; Kavanaugh, J. S.; Triplett, K. D.; Figueroa, M.; Raja, H. A.; El-Elimat, T.; Crosby, H. A.; Femling, J. K.; Cech, N. B.; Horswill, A. R.; Oberlies, N. H.; Hall, P. R.  $\omega$ -Hydroxyemodin Limits *Staphylococcus Aureus* Quorum Sensing-Mediated Pathogenesis and Inflammation. *Antimicrob. Agents Chemother.* **2015**, *59* (4), 2223–2235. <https://doi.org/10.1128/AAC.04564-14>.
- (27) Paguigan, N. D.; El-Elimat, T.; Kao, D.; Raja, H. A.; Pearce, C. J.; Oberlies, N. H. Enhanced Dereplication of Fungal Cultures via Use of Mass Defect Filtering. *J. Antibiot. (Tokyo)* **2017**, *70* (5), 553–561. <https://doi.org/10.1038/ja.2016.145>.
- (28) Zhang, H.; Zhang, D.; Ray, K.; Zhu, M. Mass Defect Filter Technique and Its Applications to Drug Metabolite Identification by High-Resolution Mass Spectrometry. *J. Mass Spectrom.* **2009**, *44* (7), 999–1016. <https://doi.org/10.1002/jms.1610>.
- (29) Xie, T.; Liang, Y.; Hao, H.; A, J.; Xie, L.; Gong, P.; Dai, C.; Liu, L.; Kang, A.; Zheng, X.; Wang, G. Rapid Identification of Ophiopogonins and Ophiopogonones in Ophiopogon Japonicus Extract with a Practical Technique of Mass Defect Filtering Based on High Resolution Mass Spectrometry. *J. Chromatogr. A* **2012**, *1227*, 234–244. <https://doi.org/10.1016/j.chroma.2012.01.017>.
- (30) Pan, H.; Yang, W.; Yao, C.; Shen, Y.; Zhang, Y.; Shi, X.; Yao, S.; Wu, W.; Guo, D. Mass Defect Filtering-Oriented Classification and Precursor Ions List-Triggered High-Resolution Mass Spectrometry Analysis for the Discovery of Indole Alkaloids from *Uncaria Sinensis*. *J. Chromatogr. A* **2017**, *1516*, 102–113. <https://doi.org/10.1016/j.chroma.2017.08.035>.
- (31) Sleno, L. The Use of Mass Defect in Modern Mass Spectrometry. *J. Mass Spectrom.* **2012**, *47*, 226–236. <https://doi.org/10.1002/jms.2953>.
- (32) Amrine, C. S. M.; Raja, H. A.; Darveaux, B. A.; Pearce, C. J.; Oberlies, N. H. Media Studies to Enhance the Production of Verticillins Facilitated by in Situ Chemical Analysis. *J. Ind. Microbiol. Biotechnol.* **2018**, *45* (12), 1053–1065. <https://doi.org/10.1007/s10295-018-2083-8>.
- (33) Maharachchikumbura, S. S. N.; Guo, L.-D.; Chukeatirote, E.; Bahkali, A. H.; Hyde, K. D. Pestalotiopsis—Morphology, Phylogeny, Biochemistry and Diversity. *Fungal Divers.* *50* (1), 167–187.
- (34) Xu, J.; Yang, X.; Lin, Q. Chemistry and Biology of Pestalotiopsis-Derived Natural Products. *Fungal Divers.* **2014**, *66* (1), 37–68. <https://doi.org/10.1007/s13225-014-0288-3>.
- (35) Ding, G.; Li, Y.; Fu, S.; Liu, S.; Wei, J.; Che, Y. Ambuic Acid and Torreyanic Acid Derivatives from the Endolichenic Fungus *Pestalotiopsis* Sp. *J. Nat. Prod.* **2009**, *72* (1), 182–186. <https://doi.org/10.1021/np800733y>.

- (36) Zhang, H.; Zhu, M.; Ray, K. L.; Ma, L.; Zhang, D. Mass Defect Profiles of Biological Matrices and the General Applicability of Mass Defect Filtering for Metabolite Detection. *Rapid Commun. Mass Spectrom.* **2008**, *22* (13), 2082–2088. <https://doi.org/10.1002/rcm.3585>.
- (37) Stagliano, M. C.; DeKeyser, J. G.; Omiecinski, C. J.; Jones, A. D. Bioassay-Directed Fractionation for Discovery of Bioactive Neutral Lipids Guided by Relative Mass Defect Filtering and Multiplexed Collision-Induced Dissociation. *Rapid Commun. Mass Spectrom.* **2010**, *24* (24), 3578–3584. <https://doi.org/10.1002/rcm.4796>.
- (38) Stratton, T. Delivering Confidence for Small Molecule Identification. ThermoScientific, White paper 65374, 10. <https://assets.thermofisher.com/TFS-Assets/CMD/Reference-Materials/wp-65374-ms-mzcloud-libraries-wp65374-en.pdf>
- (39) Todd, D. A.; Parlet, C. P.; Crosby, H. A.; Malone, C. L.; Heilmann, K. P.; Horswill, A. R.; Cech, N. B. Signal Biosynthesis Inhibition with Ambuic Acid as a Strategy to Target Antibiotic-Resistant Infections. *Antimicrob. Agents Chemother.* **2017**, *61* (8), e00263-17. <https://doi.org/10.1128/AAC.00263-17>.
- (40) Otto, M. Basis of Virulence in Community-Associated Methicillin-Resistant *Staphylococcus Aureus*. *Annu. Rev. Microbiol.* **2010**, *64* (1), 143–162. <https://doi.org/10.1146/annurev.micro.112408.134309>.

APPENDIX A

SUPPLEMENTARY DATA

<b>Figure S1. Molecular Structure of Ambuic Acid .....</b>	<b>40</b>
<b>Figure S2. <sup>1</sup>H NMR Spectrum of Ambuic Acid Isolated from <i>P. microspora</i> .....</b>	<b>41</b>
<b>Figure S3. <sup>13</sup>C NMR Spectrum of Ambuic Acid Isolated from <i>P. microspora</i> .....</b>	<b>42</b>
<b>Figure S4. <sup>1</sup>H NMR Spectrum of an Analog Isolated from <i>P. microspora</i> .....</b>	<b>43</b>
<b>Figure S5. Mass Defect Filtering Workflow Chart.....</b>	<b>44</b>
<b>Figure S6. Figure S6. G910-18012-54 Recovered Masses.....</b>	<b>45</b>
<b>Figure S7. Figure S7. G910-18012-75 Recovered Masses. ....</b>	<b>46</b>

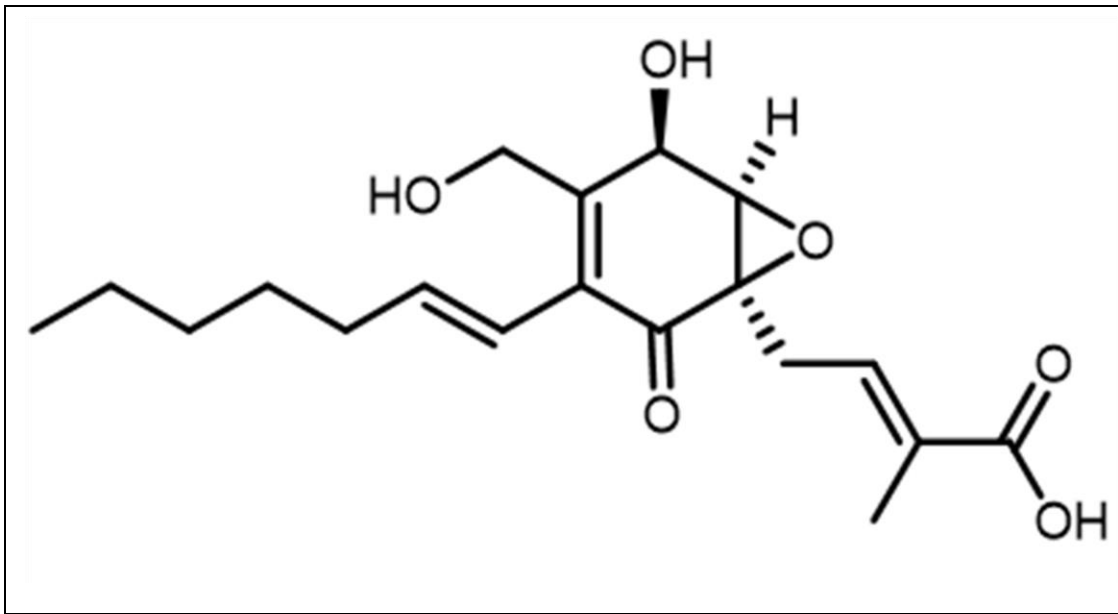


**Figure S1. Molecular Structure of Ambuic Acid.**

G910-18012-68-II  
single\_pulse

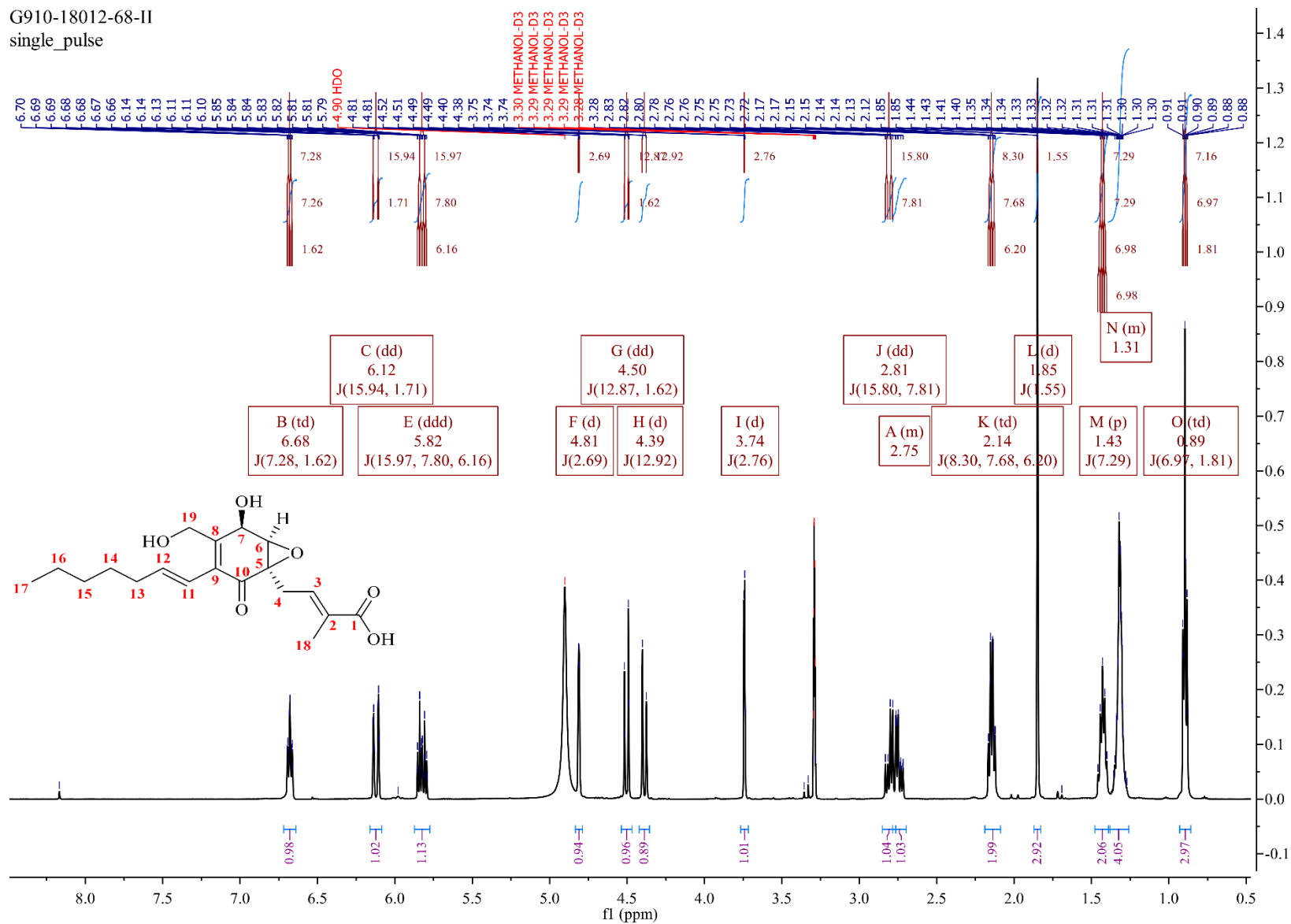


**Figure S2. <sup>1</sup>H NMR Spectrum of Ambuic Acid Isolated from *P. microspora*.** <sup>1</sup>H NMR (68-II, 500 MHz; CD<sub>3</sub>OD) Spectrum of ambuic acid isolated from cultures of *P. microspora* via preparative HPLC. G910- represents the fungal isolate code, while 18012-68, represents the notebook number and page. II is the fraction ID.

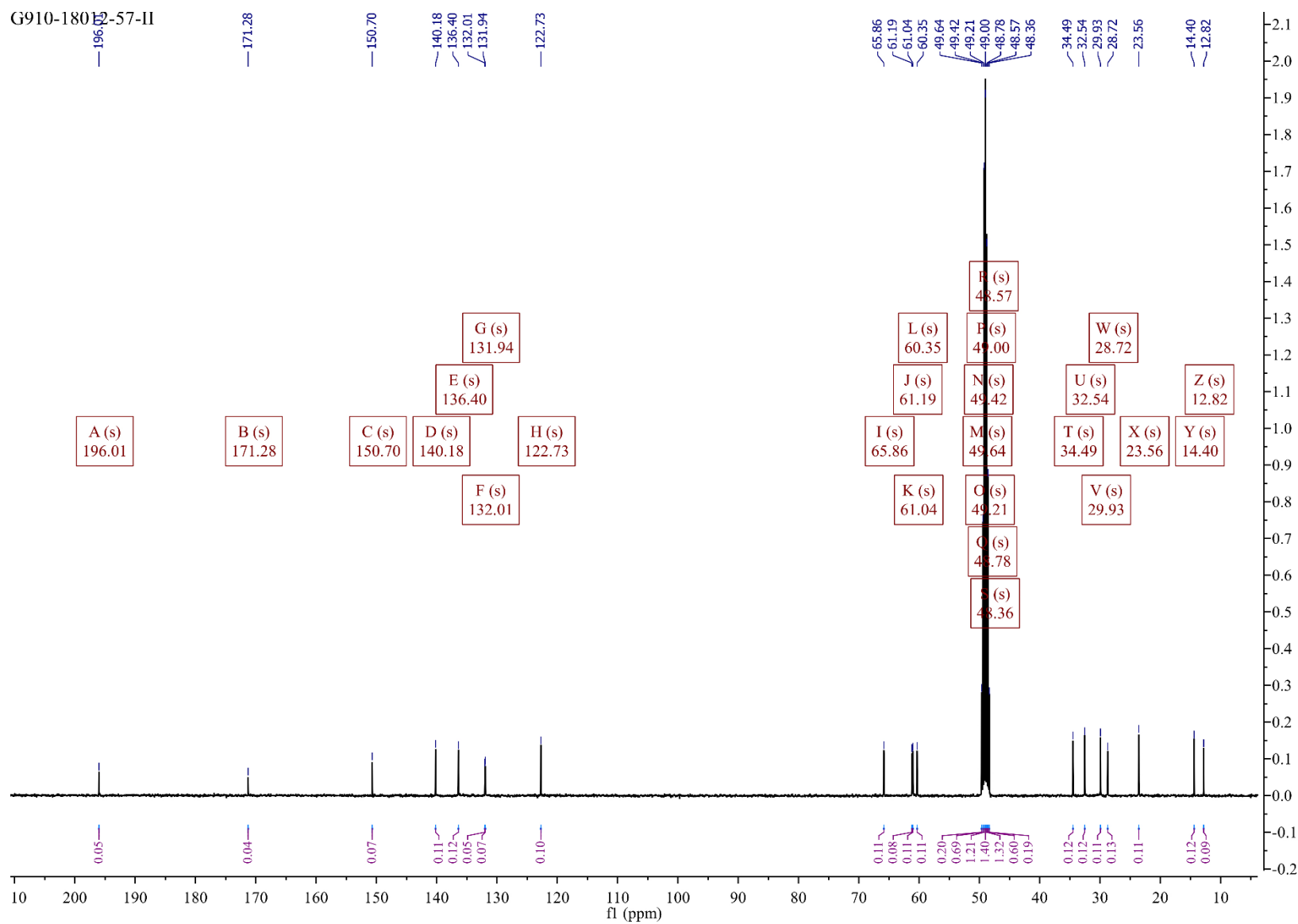


**Figure S3.**  $^{13}\text{C}$  NMR Spectrum of Ambuic Acid Isolated from *P. microspora*.  $^{13}\text{C}$  NMR Spectrum (125 MHz;  $\text{CD}_3\text{OD}$ ) of ambuic acid isolated from *P. microspora* via preparative HPLC. G910- represents the fungal isolate code, while 18012-57, represents the notebook number and page. II is the fraction ID.



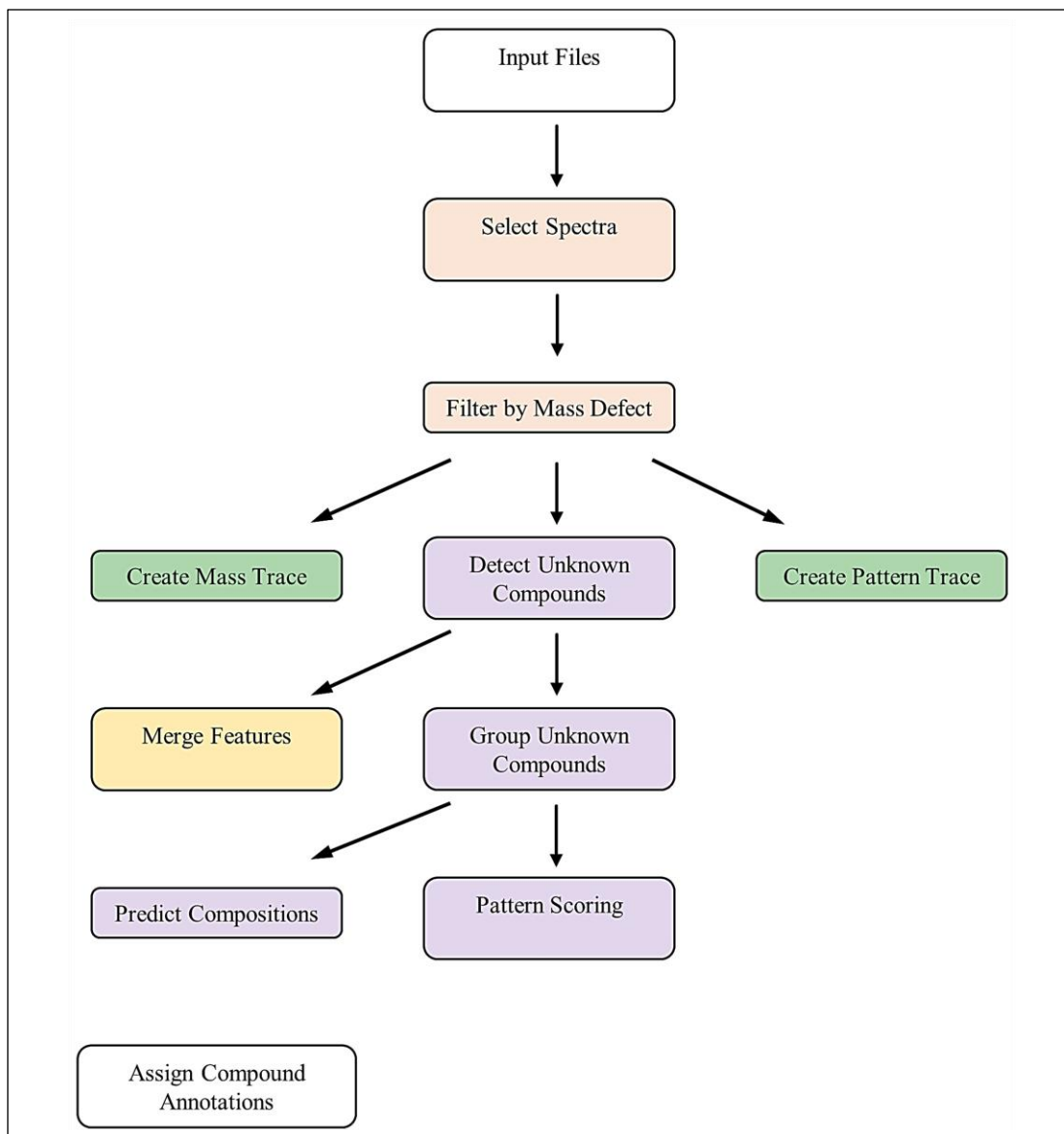


**Figure S5. Mass Defect Filtering Workflow Chart.** A filter for centroid peaks in  $MS^1$  spectra was set for mass defect ranges calculated from ambuic acid's molecular formula composition,  $C_{19}H_{26}O_6$ , with  $m/z$  tolerance set at 500 Da and mass defect tolerance of 50 mDa. Negative polarity base peak chromatograms set to be isolated within 5ppm and isotopic pattern created, with detected unknown compounds in the data using Component Elucidator Algorithm. All the detected compounds were set to be grouped by molecular weight and retention time across all files.

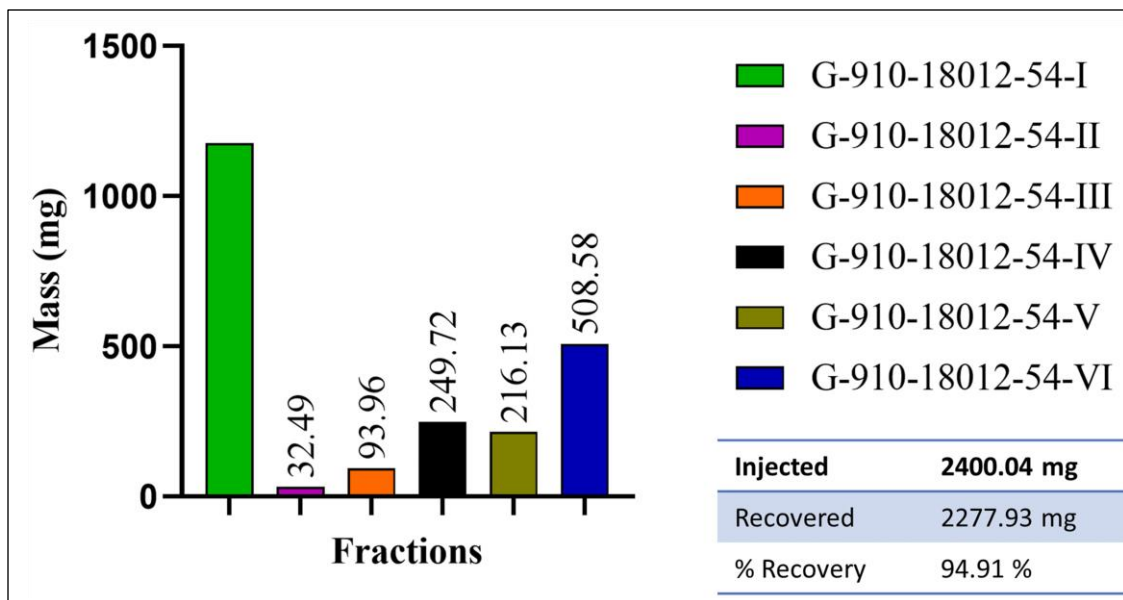


**Figure S6. G910-18012-54 Recovered Masses.** The bar graph represents the recovered masses of fractions collected from fractionation of the combined replicate biological extracts, SM-002, SM-003 and SM-004. The fractions are identified by the fungal strain number-910, notebook number 18012, and page and fraction number 54-I through 54-VI. Percent recovery was calculated from the formula: % recovery =  $\frac{\text{Recovered}}{\text{Injected}} \times 100$ . The masses are in milligrams.

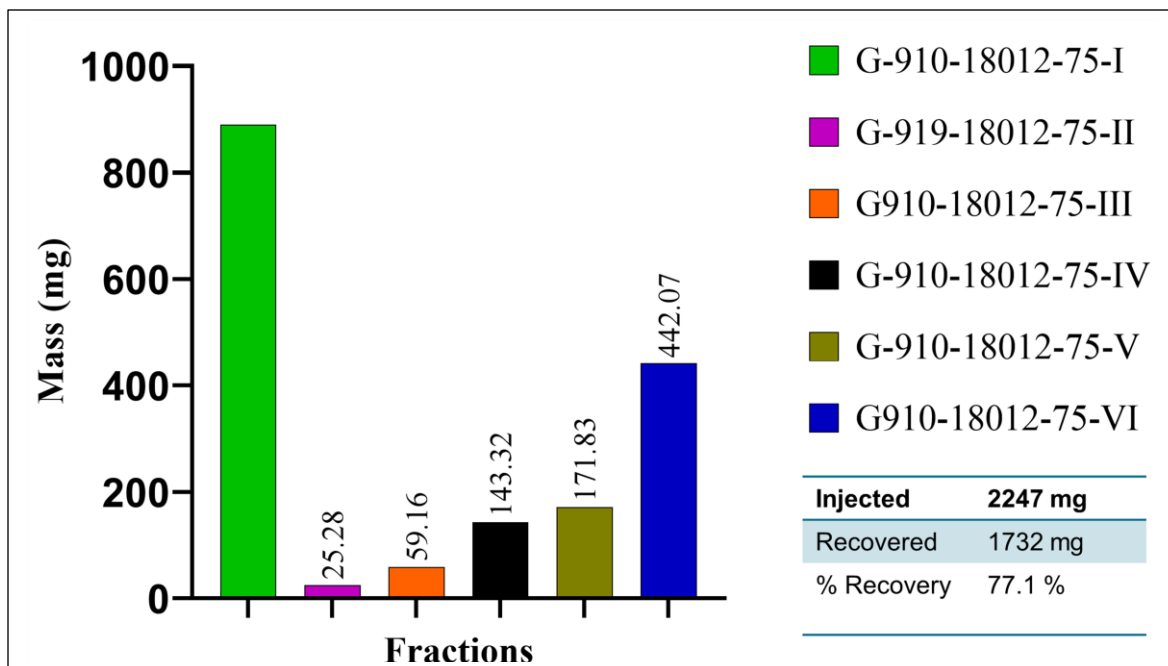


**Figure S7. G910-18012-75 Recovered Masses.** The bar graph represents the recovered masses of fractions collected from fractionation of the combined replicate biological extracts, SM-005, SM-006 and SM-007. The fractions are identified by the fungal strain number-910, notebook number 18012, and page and fraction number 75-I through 75-VI. Percent recovery was calculated from the formula: % recovery = Recovered/Injected  $\times$  100. The masses are in milligrams.